Ana Catarina Alves Bastos

Degree in Biochemistry

Modulation of neuroinflammation by phenolic sulfates metabolites

Dissertation to obtain a Master Degree in Biochemistry for Health

Supervisor: Cláudia Nunes dos Santos, PhD, iBET/ITQB-UNL

December, 2017

Ana Catarina Alves Bastos

Degree in Biochemistry

Modulation of neuroinflammation by phenolic sulfates metabolites

Dissertation to obtain a Master Degree in Biochemistry for Health

Supervisor: Cláudia Nunes dos Santos, PhD, iBET/ITQB-UNL

Júri:
Presidente: Prof. Doutor Pedro Matias
Arguente: Prof. Doutora Teresa Pais
Vogal: Prof. Doutora Margarida Archer

Instituto de Tecnologia Química e Biológica António Xavier

December, 2017

Modulation of neuroinflammation by phenolic sulfates metabolites

AGRADECIMENTOS

O meu primeiro agradecimento vai naturalmente para a minha Orientadora, Dr.ª Cláudia Nunes dos Santos, por todo o apoio e ajuda disponibilizados ao longo de todo este ano. Ensinou-me a sabedoria de enfrentar os obstáculos e as dificuldades com os quais me ia confrontando, assim como a melhor forma de os contornar, sem nunca descuidar o rigor e a realidade inerentes a cada um.

Um obrigado especial também a cada elemento do inolvidável grupo do Laboratório Molecular Nutrition and Health (MNH) que me acompanhou e acolheu ao longo do meu percurso de estágio, sem os quais, o enriquecimento das minhas competências não teria sido definitivamente o mesmo. Andreia Gomes, agradeço-te os conselhos sábios nos momentos certos e toda a interação que estabelecemos quando me transmitiste parte do empenhamento e profissionalismo que hoje me carateriza. Inês Figueira, uma enorme gratidão pela tua ajuda incondicional e por todos os ensinamentos e sorrisos que me proporcionaste em cada etapa que fui ultrapassando. Joana Pereira, obrigada pela boa disposição que te caracteriza e por todo o otimismo que me transmitias nos momentos mais difíceis. Rita Ramos, a ti agradeço-te por toda a disponibilidade ao longo destes meses; a tua enorme sabedoria foi parte essencial de muitas das conquistas que alcancei. Dr.ª Regina Menezes e Dr.ª Paula Pinto, o meu sincero obrigado também pelo Exemplo que me transmitiram. Um especial obrigado a ti Gonçalo Garcia, que, sem as bases chave que me transmitiste não teria conseguido tocar o patamar que hoje atingi - muitas das conquistas que alcancei devo-as a ti.

Quero também agradecer às colegas que iniciaram o estágio de mestrado no mesmo laboratório e no mesmo período que eu, e com quem partilhei as mais incríveis experiências e aprendizagens. Obrigada Filipa Félix e Marcela Vaz, pela constante boa disposição e pelo companheirismo.

Um obrigado também aos sempre presentes meus grandes amigos que me apoiaram nesta minha caminhada, que dita o término de mais uma etapa de especial importância na minha vida, e na minha futura carreira profissional. Irmãs, a vocês que me acompanham desde os meus 10 anos, obrigada pela compreensão e pelo apoio incondicional em todos os momentos que culminaram nesta fase. Francisco Mendonça, obrigada por toda a força e coragem que me transmitiste. Joana Gonçalves, a ti ser-te-ei eternamente grata por todos os minutos que me acompanhaste e aconselhaste incondicionalmente nos momentos mais complicados; foste e és um dos meus maiores pilares.

Aos meus pais, e especialmente ao meu querido irmão, quero neste momento deixar um indelével agradecimento por todo o apoio e enorme vontade demonstrada em me proporcionar o melhor para o meu futuro, durante estes largos anos. Sem vocês eu nunca teria conseguido chegar onde cheguei e alcançar o que alcancei. Foram essenciais em todo o percurso da minha vida académica, sendo por isso a parte essencial da pessoa que me tornei e da qual muito me orgulho. Eu sou uma grande parte de vós.

Um especial obrigado a todos vós!

"Every accomplishment starts with the decision to try."

John F. Kennedy

ABSTRACT

Within the central nervous system, microglial cells are key regulators of a set of inflammatory processes. The microglial inflammatory response is the main contributor to the process of neuroinflammation. Inside the brain, under certain abnormal conditions, a sustained microglial activation may lead to an exacerbation of the inflammatory state, causing chronic pathological conditions such as neurodegeneration.

The occurrence of neurodegenerative disorders has been steadily increasing, with no cure currently available. Thus, there is an urgent need to find ways to prevent or at least slow the progression of these diseases. Epidemiological studies demonstrate that a diet rich in (poly)phenols (fruits and vegetables) reduces the risk of developing several diseases, including neurodegenerative diseases.

The aim of the present study is to investigate the modulation of neuroinflammation by two bioavailable (poly)phenol metabolites, Catechol-O-sulfate (Cat-sulf) and Pyrogallol-O-sulfate (Pyr-sulf), in a lipopolysaccharide (LPS)-stimulated microglial cell model.

The release levels of different cellular inflammatory mediators were analyzed in parallel with specific markers also involved in the activation of the NF-κB signaling pathway. Pyr-sulf was the most promising metabolite tested, leading to a dramatic reduction of TNF-α production following LPS stimulation, at concentrations and residence times that are physiologically relevant. Pyr-sulf also showed an interesting effect by reducing IκBα phosphorylation, while simultaneously increasing basal levels of IκBα protein. Phosphorylation levels of NF-κB also appeared to be modulated by this (poly)phenol metabolite, although this effect only persisted for a short time following stimulation. In addition, under the tested conditions, the increase in NF-κB nuclear translocation, following stimulation by LPS, did not seem to be affected by Pyr-sulf pretreatment, in contrast to what was observed for IκBα phosphorylation.

This work highlights the potential of Pyr-sulf, a bioavailable (poly)phenol metabolite, as an efficient modulator of deleterious neuroinflammatory processes with a variety of possible roles for the prevention of neurodegeneration.

RESUMO

No sistema nervoso central, as células da microglia desempenham um importante papel na regulação de um vasto conjunto de processos inflamatórios, sendo a resposta inflamatória desencadeada responsável por um fenómeno denominado neuroinflamação. Perante situações anormais no cérebro, a microglia pode atingir um estado de ativação persistente associado a um estado inflamatório prolongado, resultando em situações patológicas, como por exemplo a neurodegeneração.

Uma vez que a incidência de distúrbios neurodegenerativos ainda sem cura disponível tem vindo a aumentar, surge a necessidade de encontrar formas de prevenir ou, pelo menos, diminuir a sua progressão. Estudos epidemiológicos demonstram que uma dieta rica em (poli)fenóis (frutas e vegetais) reduz o risco de desenvolver diversas patologias, incluindo doenças neurodegenerativas.

O presente trabalho tem como objetivo investigar o efeito modulador de dois metabolitos (poli)fenólicos biodisponíveis, Catechol-O-sulfate (Cat-sulf) e Pyrogallol-O-sulfate (Pyr-sulf), num modelo de neuroinflamação usando células de microglia expostas a um lipopolissacarídeo (LPS) bacteriano.

A libertação de diferentes mediadores celulares inflamatórios foi analisada em paralelo com outros marcadores específicos, envolvidos na ativação da via de sinalização do NF-κB. O Pyr-sulf surgiu como o metabolito mais promissor, mostrando uma redução acentuada nos níveis de TNF-α, após o estimulo com LPS, para concentrações e tempos de incubação com significado fisiológico. O Pyr-sulf evidenciou ainda um efeito na redução dos níveis de fosforilação da proteína IκBα, consistente com o aumento dos níveis basais da mesma. No entanto, apesar dos níveis de fosforilação do NF-κB também terem sido influenciados por este mesmo metabolito, o efeito modulatório apenas se verificou para tempos curtos de exposição ao LPS. É ainda de salientar que o aumento da translocação nuclear do NF-κB na presença do LPS parece não sofrer qualquer alteração aquando da incubação prévia com o metabolito, contrariamente ao observado para a fosforilação da proteína IκBα.

Em suma, este trabalho permitiu realçar o potencial do Pyr-sulf na modulação de processos neuroinflamatórios e a possibilidade de desempenhar um papel importante na prevenção da neurodegeneração.

Palavras-chave

Microglia, (Poli)fenóis, Neuroinflamação, NF-κB

INDEX OF CONTENTS

INDEX OF TABLES

ABBREVIATIONS

Abs	Absorbance
APC	Antigen presenting cells
Arg1	Arginase 1
ABTS	2,2'-azino-bis (3-ethylbenzothiazoline-6-sulphonic acid)
BBB	Blood-brain barrier
BSA	Bovine serum albumin
Cat-sulf	Catechol-O-sulfate
C_{max}	Maximum concentration
CNS	Central nervous system
DAMPs	Damage-associated molecular patterns
DAPI	4',6-diamidino-2-phenylindole
DEPC	Diethylpyrocarbonate
DHE	Dihydroethidium
DMSO	Dimethylsulfoxide
EMEM	Eagle minimum essential medium
ECL	Enhanced chemiluminescence
ELISA	Enzyme-linked immunosorbent assay
FBS	Fetal bovine serum
GAPDH	Glyceraldehyde 3-phosphate dehydrogenase
IKK	Inhibitor of kappa B kinase
IL	Interleukins
IκB	Inhibitory kappa B proteins
LPS	Lipopolysaccharide
MBA	Membrane blocking agent
MFI	Median fluorescence intensity
MHC	Major histocompatibility complex
NOS	Nitric oxide species
NEAA	Non-essential amino acid solution
NP-40	Nonylphenyl polyethylene glycol
NFAT	Nuclear factor of activated T-cells
NF-κB	Nuclear transcription factor kappa B
PAMPs	Pathogen-associated molecular patterns
PD	Parkinson's disease
PFA	Paraformaldehyde
PRR	Pattern recognition receptors

PBS	Phosphate buffer saline
PVDF	Polyvinylidene difluoride
Pyr-sulf	Pyrogallol-*O*-sulfate
RIPA	Radioimmunoprecipitation assay
ROS	Reactive oxygen species
RT	Room temperature
SDS	Sodium dodecyl sulfate
TAD	Carboxy-terminal transactivation domain
TIR	Toll/interleukin 1 receptor
TLR	Toll-like receptors
TGF-β	Transforming growth factor β
TBST	Tris-buffered saline with Tween20
TNF-α	Tumor necrosis factor-alpha

OBJECTIVES

Previous results from the *Molecular Nutrition and Health Laboratory* have demonstrated the potential neuroprotective effect of two different human bioavailable (poly)phenol metabolites. Both Catechol-*O*-sulfate (Cat-sulf) and Pyrogallol-*O*-sulfate (Pyr-sulf) reduced common hallmarks of neurodegeneration such as increased oxidative stress, neuronal excitotoxicity and neuroinflammation. In a lipopolysaccharide (LPS)-stimulated N9 microglial cell model, Pyr-sulf had shown significant attenuation of neuroinflammatory responses, mainly through the regulation of NF-κB nuclear import and the modulation of IκBα protein levels.

The aim of the present study, performed in the same model cell system, was focused on elucidating the potential of these two physiological (poly)phenol metabolites to modulate the microglial neuroinflammatory response. The experimental work was divided into two major tasks, performed in parallel, based on a pretreatment approach under physiological conditions. In a previous human bioavailability study performed by our laboratory, the maximum plasma concentration and the time during which the Cat-sulf and Pyr-sulf metabolites were in circulation was determined.

In the first task, the effects of the dose and incubation times of these (poly)phenol metabolites were analyzed, at lower concentrations and for shorter residence periods than were previously used. This task was focused on the analysis of the profile of both pro and anti-inflammatory mediators, in microglia cells activated with LPS following a pretreatment with Pyr-sulf and Cat-sulf metabolites.

The second task was based on the analysis of one of the most crucial signaling cascades activated upon LPS stimulation, the NF-κB signaling pathway. The NF-κB pathway regulates the transcription of a diverse range of target genes as part of an inflammatory response. The effects of Pyr-sulf on specific protein markers from this pathway were evaluated. Specifically, the protein levels and phosphorylation state of NF-κB and its inhibitor, IκBα, as well as the translocation of the NF-κB transcription factor into the nucleus.

1. STATE OF THE ART

1.1 Neuroinflammation: a central nervous system response

1.1.1 Molecular and cellular features of the central nervous system

The central nervous system (CNS) consists of the brain and the spinal cord and comprises a key part of the nervous system[1]. The ability of the CNS to control a variety of cellular mechanisms, including important immune responses, has been extensively described: the major role of the CNS is to restore and to maintain homeostasis inside the brain.

Over the years, the CNS has been considered as isolated, protected from a diverse range of external factors by the blood-brain barrier (BBB). The BBB restricts, among other factors, the access of peripheral immune components. Due to such tight control, the CNS possesses its own resident immune elements – the microglia cells – responsible not only for neuronal maintenance but also for an essential surveillance role[2,3]. Their capacity to trigger a wide range of inflammatory responses to a plethora of either external or internal factors, such as traumas, strokes, injuries, toxins, disease-related endogenous proteins and neuronal damage, makes them important components of the innate immune system inside the CNS. In this regard, microglial activation, along with other cellular mediators, plays an important role in the regulation of neuroinflammation and in the repair of the neuronal microenvironment.

Taking all of this into account, and looking at current research, the linkage between the nervous and immune systems is starting to be revealed. This linkage may begin to explain the origins of certain pathological processes related with neurological disorders, including degenerative disorders such as Alzheimer's disease, Parkinson's disease (PD) and amyotrophic lateral sclerosis[3,4].

1.1.2 Inflammatory status and mediators profile

Within the CNS, the cytokine networks play an important role in cellular organization, acting as both growth and survival factors. Their function in the differentiation of neuronal and glial cells, and their ability to regulate cellular communication, make them crucial mediators. Maintenance of cytokine levels is imperative to maintain homeostasis. A disruption of balance within the cytokine network can act as a very strong effector, not only at the tissue level but also as part of a global inflammatory state[5].

Dysregulation of the cellular functionalities within the CNS initiates an immediate inflammatory response that can be associated with neuroinflammatory or neurodegenerative conditions. Inflammatory diseases and infections are related with a common blood-borne influx of myeloid cells and lymphocytes into the brain, promoted by an increase of BBB permeability (**Figure 1.1**)[5]. Invading immune cells, acting as the main source of mediators, trigger a tissue response with the production of pro-inflammatory markers, such as tumor necrosis factor-alpha (TNF-α), interleukins IL-6 and IL-1, reactive oxygen species (ROS) and nitric oxide (NO) species. The delivery of these mediators into the CNS activates

glial cells further raising the production of pro-inflammatory markers, thus exacerbating the inflammatory state. On the other hand, in the presence of a homeostatic imbalance or neuronal loss (as, for instance caused by abnormal protein aggregates which are observed in a variety of neurodegenerative conditions), the CNS begins a self-sustaining response mediated by its own resident cells and where invading immune cells make only a minimal contribution (**Figure 1.1**)[5]. Both responses are characterized by a perturbation of homeostasis and the production of excess pro-inflammatory mediators that may compromise cellular viability. Thus, a switch to an anti-inflammatory state, guided by IL-10, IL-4, TGF-β cytokines and neurotrophic factors, is crucial to efficiently repair tissue damage and to restore the mediators to normal levels, thus downregulating the inflammation[6,7].
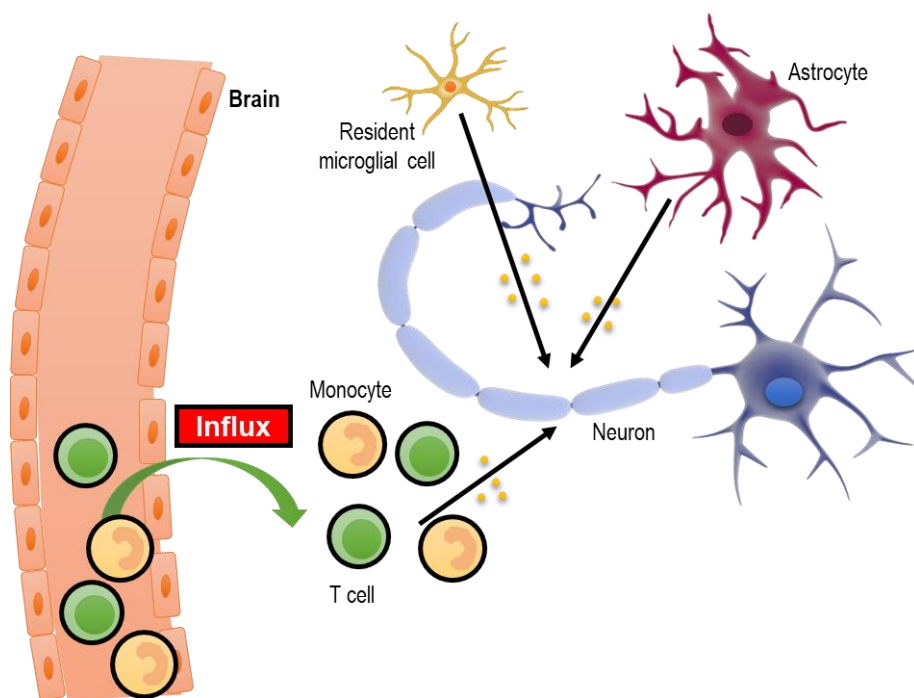
Figure 1.1. Neuroinflammatory conditions and the contribution of invading immune cells. Inflammatory diseases and infection are commonly associated with a blood-borne influx of myeloid and lymphocyte cells to the CNS parenchyma. Production of mediators activate glial cells to perpetuate the inflammatory state towards tissue damage.
Figure adapted from B. Becher, S. Spath, J. Goverman, Nature Reviews (2016).

1.2   Microglia, the active surveilling resident immune cells

Microglia represent essential elements of the CNS immune neuroglia network which comprise all non-neuronal cells present in the brain and spinal cord, like astrocytes, oligodendrocytes and ependymal cells[4]. Microglia cells have been reported as one of the most important cellular components of the CNS. Microglia play a determinant role in brain homeostasis and in neuronal maintenance. They are also involved in brain dysfunctions leading to pathological conditions.

Microglia cells are derived from myeloid precursor cells, representing 5-20% of all glial cells present in the CNS and described as the most abundant mononuclear phagocytes[8]. Additionally, it is currently accepted that these cells are characterized by a functional and morphological heterogeneity, having the versatility to respond to different stimulus types and share some features with other tissue-resident macrophages[9].

1.2.1   Microglial morphology in healthy and disease states

As the resident immune cells of the CNS, microglia are known to be the first line of defense against any threat or damage, ranging from responses to simple neuronal dysfunctions all the way up to huge brain abnormalities.

In a normal, healthy brain, microglia cells appear with multiple cellular extensions characterized by a branched morphology. Such a phenotype is clearly observed in a "resting" state when microglia perform an immune-surveillance role that controls large brain regions[10,11]. When an injury is detected, microglia become activated leading to specific cellular modifications. A morphological change into an amoeboid shape is associated with a high phagocytic capacity and by an intensification of the inflammatory process. It is increasingly accepted that these two morphological states represent extreme microglial phenotypes. Their morphological behavior is more subtle than this simple two-state model and there is huge heterogeneity within the microglial activation spectrum[12].

1.2.2   Microglia activation paradigm

The complexity behind microglia activation states is linked to different stimuli that determine their neurotoxic or neuroprotective cellular functions. For instance, following a lipopolysaccharide (LPS) stimulation activated microglia become neurotoxic releasing a range of pro-inflammatory mediators such as IL-1β, TNF-α, ROS and NO. Such mediators play a key role in cell defense, killing invading organisms and leading to an exacerbation of the inflammatory condition. On the other hand, the neuroprotective function that is promoted by cytokine signals like IL-4 and IL-10, inhibits the microglial neurotoxic function. During the neuroprotective state, microglia are focused on reversing the inflamed state by releasing anti-inflammatory markers such as IL-10, IL-4, Arginase 1 (Arg1) and transforming growth factor β (TGF-β)[9,13,14] (**Figure 1.2**). A proper transition between these neurotoxic

and neuroprotective microglial responses, known as classic activation and alternative activation, respectively, leads to the reestablishment of cellular homeostasis.
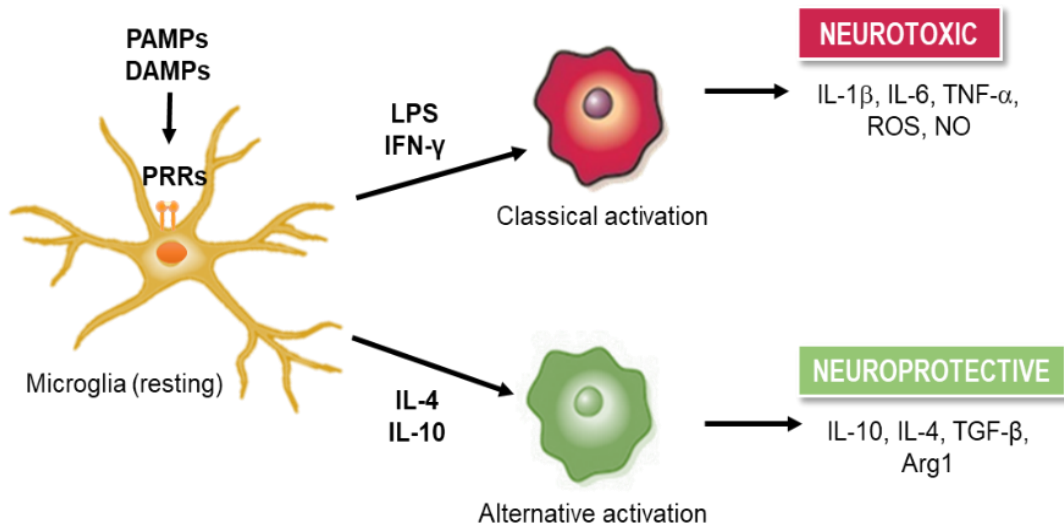
Figure 1.2. Microglial activation response and corresponding cellular functions. Microglial cells became activated in response to different signals which determine their subsequent neurotoxic and neuroprotective cellular functions.
Figure adapted from Y. Nakagawa, K. Chiba, Pharmaceuticals (2014).
PAMPs, Pathogen-Associated Molecular Patterns; DAMPs, Damage-Associated Molecular Patterns; PRRs, Pattern Recognition Receptors.

1.2.3   Immune molecular receptors

In addition to morphological changes and a gain of phagocytic functions in the presence of threats or damage, activated microglial cells are able to upregulate a wide range of immune sensors, known as cellular receptors. Their activation, triggered either by diverse endogenous (damage-associated molecular patterns- DAMPs) or exogenous (pathogen-associated molecular patterns- PAMPs) signals, plays a vital role in the inflammatory cascade process[15].

Under steady-state conditions, microglial cells express pattern recognition receptors (PRR) at low levels. PRRs are a huge family of diverse receptors, responsible for initiating a neurotoxic or a neuroprotective immune response in the presence of a stimulus[16]. Under pathological circumstances, a wide range of surface receptors are highly expressed, including the major histocompatibility complex (MHC) classes I and II. Because of this, microglia are considered effective antigen presenting cells (APC) in the CNS, and link the innate and adaptive immune responses[3,17]. Another important group of surface receptors are the toll-like receptors (TLRs) that recognize a variety of stimuli, promoting the regulation of inflammatory pathways and subsequent transcription activation of inflammatory mediators. In mammals, the TLR family consists of twelve members. Microglia are reported to express

only nine members, from TLR1 to TLR9[16]. Considering their upregulated expression under inflammatory conditions, these receptors become important cellular factors for recognizing PAMPs and DAMPs. Integration of these signals plays a crucial role in both healthy and damaged brain environments[18,19].

1.2.4   Nuclear transcription factor kappa B (NF-κB) signaling pathway

The interaction between a stimulus and a membrane receptor rapidly triggers a signal transduction cascade that consists of a series of phosphorylation reactions.

The nuclear transcription factor kappa B (NF-κB) cascade is one of the most important signaling pathways involved in the microglial inflammatory condition. NF-κB represents a family of monomeric transcription factors: p65(RelA); RelB; c-Rel; p105/p50 (NF-κB1); and p100/52 (NF-κB2)[20]. These monomeric transcription factors combine to form active dimeric complexes. The most abundant heterodimer present in many different cell types is p50/65[20]. Other dimer complexes have also been reported including: p65/p65, p65/c-Rel, p65/p52, c-Rel/c-Rel, p52/c-Rel, p50/c-Rel, p50/p50, RelB/p50 and RelB/p52[20].

One of the key regulatory steps involved in the activation of the NF-κB pathway is the inhibitor of kappa B kinase (IKK) complex. IKK consists of different subunits with specific cellular functions (IKKα, IKKβ and IKKγ). Under normal conditions, NF-κB dimers, such as the p65/p50 complex, are retained in the cytoplasm in an inactivated form through association with inhibitory kappa B (IκB) proteins, such as IκBα. In response to an immune or stress stimulus the enzymatic IKK complex is activated and phosphorylates IκBα. Phosphorylated IκBα is then targeted for ubiquitination and subsequent proteasomal degradation. Once the inhibitor is degraded, NF-κB is released, phosphorylated and subsequently translocated into the nucleus. NF-κB binds to specific DNA targets (promoters), the transcription of several genes is altered, coding for different mediators related with cell survival and protection processes (**Figure 1.3**). Examples of proteins encoded by genes that are regulated by NF-κB are membrane receptors such as MHC molecules, cytokines, chemokines, cell adhesion molecules, regulators of apoptosis and growth factors[21].

IκBα is also upregulated by NF-κB and thus a negative feedback loop is established[22]. The establishment of this negative feedback loop is a key strategy in controlling this transcriptional pathway and provides a means by which to respond to stimulus, monitor the response and then return to homeostasis. Proper regulation of this pathway is essential in order to avoid an over-activated NF-κB state that would result in harmful consequences.
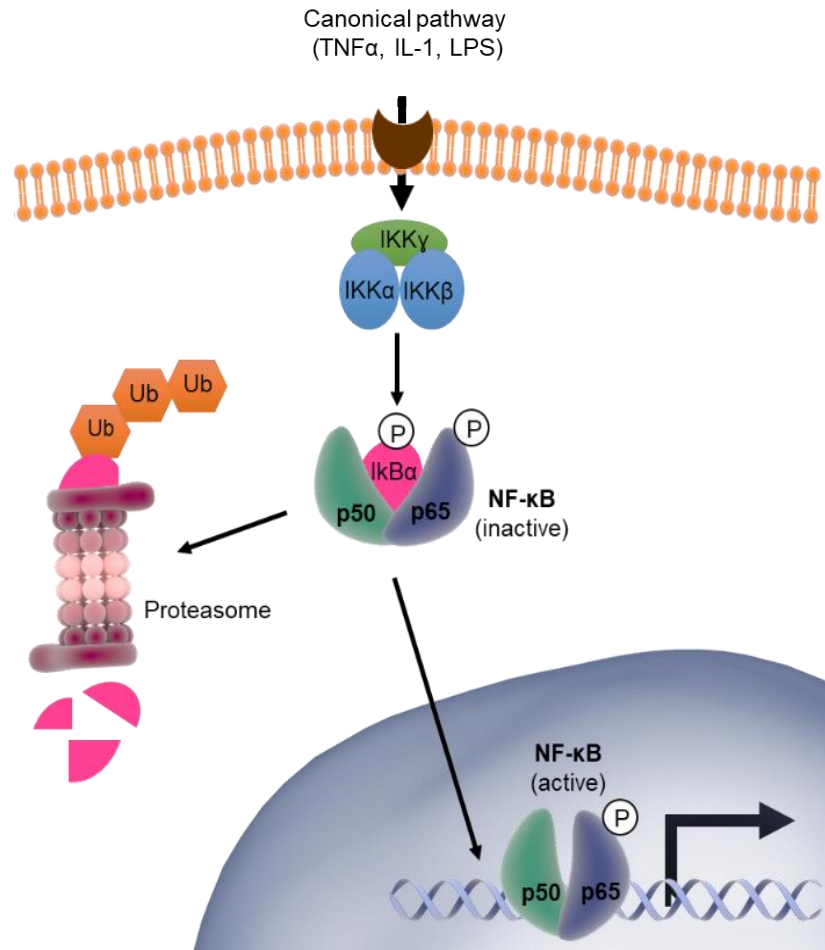
Figure 1.3. NF-κB canonical signaling pathway. Diverse stimuli are capable of activating the IKK complex with subsequent phosphorylation and degradation of the inhibitory IκBα protein. NF-κB in its free form binds to DNA regulating the expression of a plethora of genes.
Figure adapted from A. Oeckinghaus, S. Ghosh, Cold Spring Harb Perspect Biol (2009).

1.3   Neuroinflammation and diet

1.3.1   Dietary bioactives: (poly)phenols

In relatively recent times, lifestyles and dietary habits have changed greatly. These changes have been accompanied by an increase in lifetime expectancy and a concurrent increase in the incidence of chronic age-related diseases including neurodegenerative diseases[23]. Current drugs available for the treatment of most common neurodegenerative disorders are largely ineffective, only mildly alleviating the major symptoms and complications. Thus, within the scientific community, a strong motivation to find other powerful approaches to prevent or retard the development of these age-related diseases has emerged.

It is generally accepted that a healthy diet is associated with increased health and wellbeing. Thus, there is an ever increasing interest in the preventive and therapeutic effects offered by the consumption of certain compounds from natural origins[24]. Such a strategy has focused on the establishment of significant relationships between health benefits and dietary contents. In this regard, strong evidence from diverse epidemiological studies supports a clear association between the consumption of fruits and vegetables and an attenuation of several pathologies including cancers and heart disorders[25,26,27] and even an attenuation of cognitive decline[28,29,30].

From a nutritional point of view, among all diet-derived compounds, polyphenols appear as one of the most studied and powerful bioactive contributors for health. They have been extensively described not only in animal[31,32] but also in human[33,34] studies. These phenolic compounds constitute a wide and diverse group of plant-derived phytochemicals, differing from each other in terms of stability, bioavailability and biological functions[35]. Based on their origins and chemical structures, they can be organized into different classes of which the flavonoids are the largest subgroup (**Figure 1.4**)[36]. Polyphenol compounds are characterized by a common phenolic structure consisting of a linkage between at least one hydroxyl group and an aromatic ring[35]. Using the term "polyphenol" to describe these compounds may no longer be accurate, as some members possess only a single phenolic ring. Thus, in order to cover all possible phenolic structures, the correct term to use is now "(poly)phenols".

(Poly)phenols, as naturally occurring compounds, can be found in high concentrations in food sources such as: tea; coffee; cocoa; grapes; wine and berries. Berries appear to be a promising source of (poly)phenols beneficial to health. These benefits have been reported in several human nutritional studies: i) In a study using older adults with memory decline, neurocognitive benefits were observed following a daily consumption of blueberries known to be rich in anthocyanins[37]; ii) In an intervention study with healthy male volunteers, an improvement of vascular function was associated with an acute consumption of blueberries[38]; and also iii) a higher intake of flavonoids and a berry-rich diet, in both male and female volunteers, has been associated with a lower risk of developing PD[39].

All these studies provide strong support to the idea that berries' (poly)phenols and their derived compounds have a powerful effect on health and mediating age-related complications.
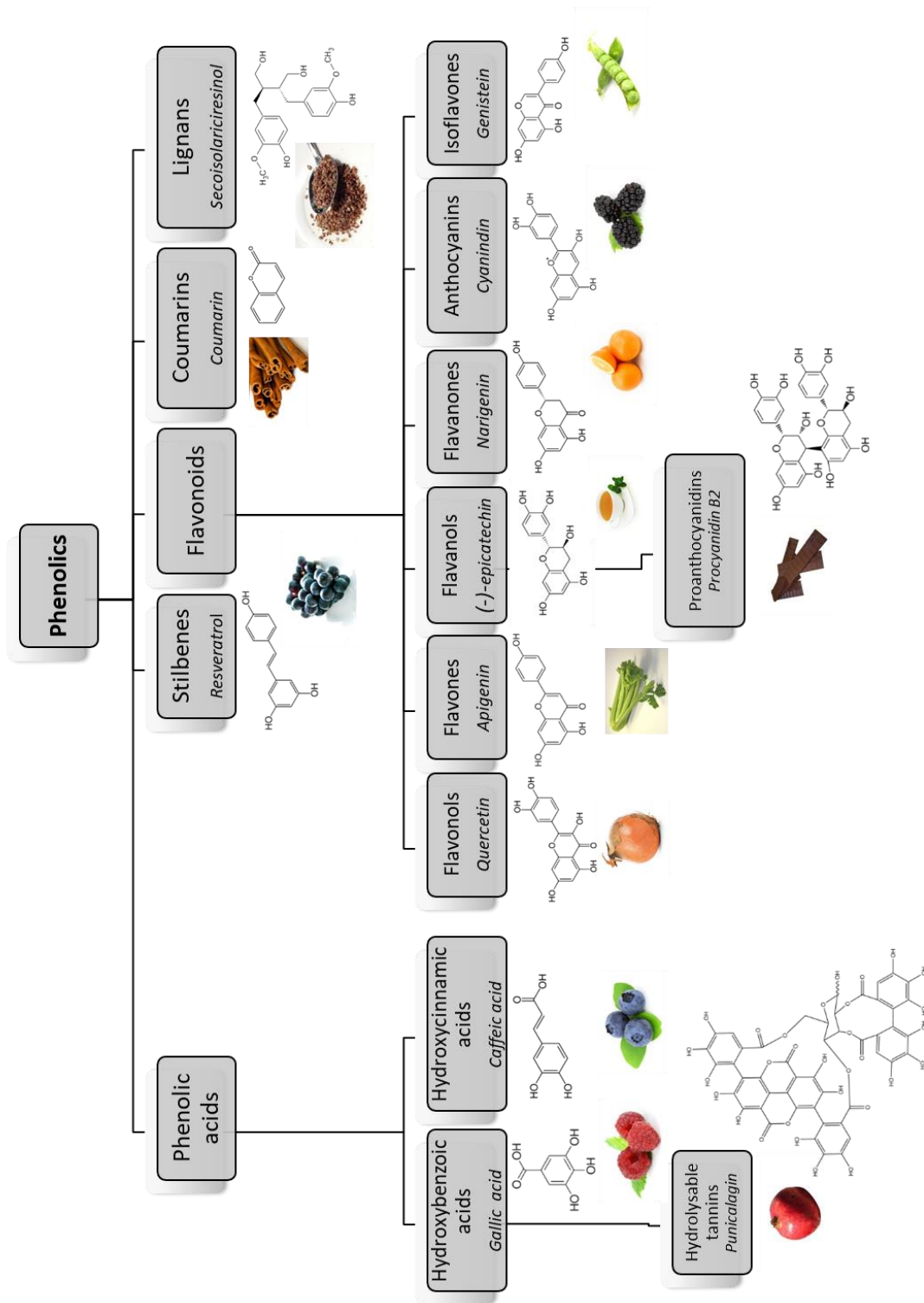
Figure 1.4. Most important diet-derived polyphenol compounds' classes. Correspondent structure, name (in italic) and food sources.
Figure from I. Figueira, R. Menezes, D. Macedo, I. Costa, C.N. Santos, Current Neuropharmacology (2017).

1.3.2   Bioavailability of phenolic compounds

Evidence from *in vitro* cellular models as to the beneficial effects of (poly)phenol compounds have generated a great deal of interest human consumption of these compounds from natural sources. However, the use of these compounds as they occur in the diet in the *in vitro* assays have been raising several doubts due to their lacking of physiological relevance. The physiological relevance of (poly)phenol concentrations and derived metabolites that can be achieved through consumption of natural sources have emerged[40]. The bioavailability of (poly)phenols *in vivo* is a crucial factor to consider for a reliable and translatable *in vitro* study. The native form of these compounds, *in vivo*, once ingested within a food matrix, undergoes several biological transformation processes. Thus, tissues may not be exposed to the (poly)phenols which were ingested but rather to their derived metabolites[40].

A compilation of all modifications that occur both during and after the digestive process must take into account all of the dynamic systems involved, as well as the corresponding metabolic reactions. Ingestion, digestion, absorption, distribution, hepatic and colonic metabolism and excretion comprise the main steps involved in the metabolic processing of (poly)phenol compounds (**Figure 1.5**)[36]. In each of these stages different chemical modifications occur, resulting in bioavailable metabolites that are different from their respective diet-derived parent compounds. Such differences are related with molecular structures, stability and biological functions of compounds, that directly influence their bioavailability and respective absorption[41]. In the case of (poly)phenols, many of these compounds occur in the diet as glycosides[40].

The oral cavity represents the first contact of the human body with different dietary elements, where the first chemical and biochemical reactions of dietary (poly)phenols take place. The major factor is the action of digestive enzymes such as amylases and proteases, which together with pH and temperature changes, leads to a reduction of particle size[41]. Mechanical action and a secretion of gastric fluids are the main mediators of the digestion stage. Moreover, the food matrix of (poly)phenols and its properties, as well the conditions within the gastrointestinal tract constitute important parameters influencing further uptake of the potentially bioavailable fraction[41]. The absorption stage occurs in the small intestine, guided by enterocyte cells, following digestion in the stomach and release of respective products (**Figure 1.5**)[36].

Unabsorbed and non-digested food components can still reach the colon and be metabolized. The large intestine has the ability to promote an extensive metabolism of ingested and digestion-derived components by a complex microbial community, generating non-polar and low molecular weight products[40]. However, absorbed gut compounds do not enter the bloodstream without going through the liver. Hepatic metabolism, also known as biotransformation, involves enzymatic systems that play different roles, grouped into phase-I and phase-II reactions[42]. The main function of this process is to convert xenobiotic compounds, such as (poly)phenols, into hydrophilic products, ensuring easy excretion. While phase-I enzymes, mainly P450 cytochromes, are responsible for introducing polar

groups into molecules, phase-II enzymes conjugate the resulting metabolites to polar compounds increasing their water solubility[42].

Such soluble metabolites may now enter the bloodstream or be eliminated in the urine, faeces and bile (**Figure 1.5**)[36]. Although some of these metabolites can then reach organs, a considerable fraction returns to the gut through the bile and is then excreted or hydrolyzed again by the microbiota and may be subjected to a subsequent colon reabsorption (enterohepatic circulation)[40].
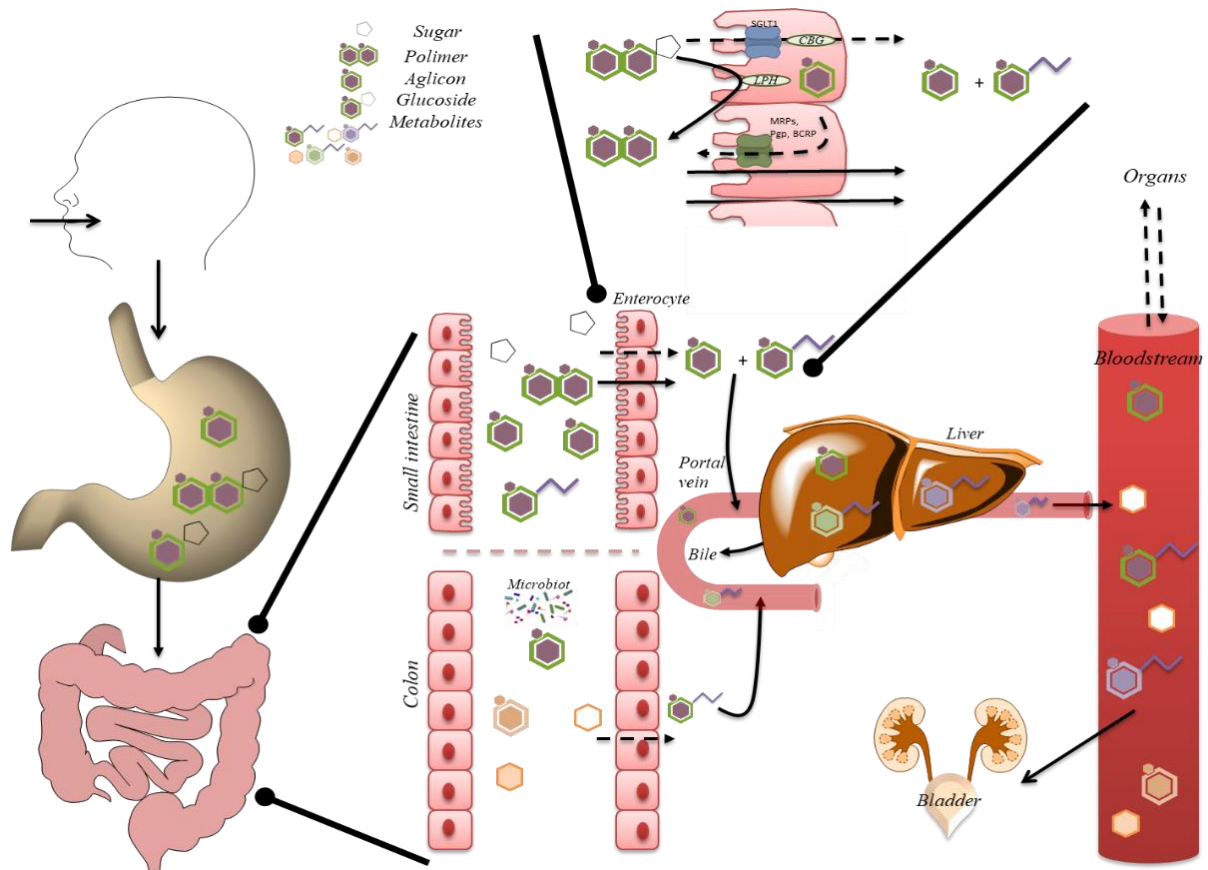
Figure 1.5. Schematic representation of the key metabolic stages of (poly)phenol compounds: ingestion, digestion, absorption, distribution, metabolism and excretion. The ingested fraction that is released by the stomach, reaches gut where some metabolites are directly absorbed and others metabolized by the colon microbial community. Once absorbed they become conjugated in the liver, being able to be secreted into the bloodstream, to be excreted or even to enter to the enterohepatic circulation.
Figure from I. Figueira, R. Menezes, D. Macedo, I. Costa, C.N. Santos, Current Neuropharmacology (2017).

The physiological relevance of metabolites, in addition to their parent compounds, is now well established. It also becomes important to look carefully for the concentration range and the period during which that these metabolites reach the circulation. The answer to these two crucial points will likely ensure a cellular responsiveness and a closer translation to an *in vivo* scenario[43].

The interplay between the colon and liver on the transformation of (poly)phenols can be measured in plasma and urine samples (products of the colonic and hepatic metabolism)[41]. Previous studies (by the group) were performed in order to detect and identify the corresponding downstream metabolites. Results from human urine samples showed increased levels of (poly)phenol metabolites in volunteers subjected to a berry-rich diet, compared with the consumption of a (poly)phenol-free meal[44]. As a result, several metabolites associated with the intake of (poly)phenols were detected and quantified for the first time. Afterwards, using human plasma samples, circulating concentrations of these metabolites were also determined, which were shown to reach micromolar levels[45]. Of all the phenolic metabolites identified, Pyrogallol-*O*-sulfate (Pyr-sulf) and Catechol-*O*-sulfate (Cat-sulf) were shown to reach the highest concentration levels, ranging from 5 to 20µM at 6 hours post-consumption, as opposed to their undetected parent compounds[45].

1.3.3 Metabolites in the brain

As already mentioned, the beneficial effects associated with the consumption of a (poly)phenol-rich diet may not be linked to just the naturally occurring compounds, but also to a wide array of new bioavailable metabolites resulting from the extensive metabolism. Such metabolites can reach relevant levels (µM levels) in the bloodstream, either by direct absorption in the small intestine or by a subsequent metabolism via hepatic enzymes and the colon microbiota[46,47]. However, the metabolites that can efficiently reach the brain, and which mechanisms are involved in their uptake through cerebral endothelial cells, the anatomical basis of the BBB, remain unclear.

Besides all the reactions and molecular transformations undergone by (poly)phenol metabolites throughout metabolic processing, the existence of physical barriers has a greater influence on their bioavailability. Such barriers constitute important lines of defense and exert tight control over uptake of metabolites. In addition to the barrier formed by enterocyte cells in the small intestine, there are others with relevant functions that must be considered such as the BBB. The latter represents a selectively dynamic structure that controls the communication between blood and the CNS, playing a protective role against pathological or harmful molecules and regulating the access of metabolites to the brain.

This brain endothelial interface is a crucial factor to take into account when determining the potential effects of (poly)phenol metabolites in the brain environment, getting as close as possible to *in vivo* events. From this perspective, some studies have suggested the brain as a possible target for (poly)phenol metabolites since measurable permeability levels across the BBB were detected in both *in vitro*[48,49, 50] and *in vivo*[51, 48, 50] models. More recently, in a study also using a BBB endothelium model

(that mimics the endothelial cells of brain capillaries), reported for the first time the ability of bioavailable phenolic sulfate metabolites, previously detected in human urine[44] and plasma[45] samples, to cross the BBB endothelium at physiologically relevant concentrations[52].

These findings have given new insights into the access of these phytochemicals to the brain. (Poly)phenol metabolites may be able to act as promising effectors, playing a crucial role at preventive brain aging conditions.

1.3.4   Promising protective role of (poly)phenols in a neuronal environment

The potential beneficial effects of (poly)phenol compounds and their derivatives have been extensively reported and described. However, many questions are still unanswered regarding their mechanism of action in the human body and particularly in a neuronal environment. Thus, currently, the greatest focus has been on cellular pathways in which (poly)phenols may be acting.

The influence of dietary (poly)phenols on different cellular hallmarks, such as the specific signaling pathways targeted, have been extensively debated. Despite the fact that some studies in animal models had shown neuroprotective effects in the presence of (poly)phenol compounds[53,54], these results became unclear once the tested compounds were used as they occur in dietary extracts. To fill this knowledge gap, some studies were carried out with (poly)phenol-derived metabolites under physiologically relevant conditions. These studies revealed neuroprotective effects reflected by a decrease in the occurrence of oxidative injury and neuronal death[55,56]. The mechanism of action of (poly)phenol metabolites may play a role in the intracellular signaling pathways underlying these effects.

The impact of phenolic compounds on several cellular pathways has suggested that different signaling mechanisms may be responsible for the resulting protective effects. For instance, despite the anti-inflammatory effect of resveratrol in modulating the cellular oxidative stress, this compound appears to be a key regulator of the β-amyloid-induced cytotoxicity state, and in addition affects different intracellular pathways, including the NF-κB cascade[57]. Moreover, the influence of these compounds on important pathways involved in a microglia-derived inflammatory state was also observed. Some dietary (poly)phenol compounds like catechin[58], luteolin[59], quercetin[60] and resveratrol[61] have been described as having a potential modulator effect on microglia activation mediated by a suppression of the NF-κB pathway. Although it has become clear that these compounds have the capacity to modulate specific cellular mechanisms, little is known about the specific role of their metabolites, after the digestion process, on a microglial inflammatory state and their true mechanism of action remains unclear.

1.4   Preliminary Results from the host laboratory

Research developed in the *Molecular Nutrition and Health (MNH) Laboratory* showed strong support for the neuroprotective potential of bioavailable phenolic sulfate metabolites, in different cell models[52]. These (poly)phenol metabolites were detected as being bioavailable in a nutritional intervention study, where urine and plasma samples from human individuals were analyzed[44,45]. From a set of metabolites identified, the correspondent circulating concentrations were determined with Pyr-sulf and Cat-sulf appearing as the most abundant metabolites.

Results from different cellular models provided clear evidence as to the neuroprotective effects of Pyr-sulf and Cat-sulf pretreatment, as well as to their ability to cross the BBB endothelial cells at circulating concentrations. Moreover, the inflammatory status of microglia cells was shown to be modulated by these metabolites, using a N9 microglial LPS-stimulated cell model, in which pro-inflammatory markers including TNF-α, intracellular superoxide, NO and CD40 receptor were evaluated. Additionally, NF-κB translocation into the nucleus and modulation of IκBα protein levels were also assessed, highlighting the potential of these (poly)phenol metabolites, mainly Pyr-sulf, in the attenuation of neuroinflammatory processes via regulation of NF-κB nuclear import and modulation of IκBα levels.
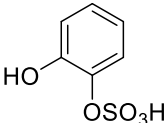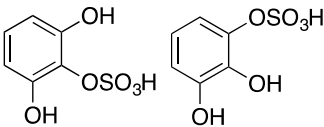
2.   MATERIALS AND METHODS

2.1   (Poly)phenol metabolites

(Poly)phenol metabolites were identified in the human plasma after a nutritional study with berry fruits[45]. In that study, their bioavailable concentrations were assessed and a range of physiological concentrations between 0.3 to 12 µM in plasma samples were observed. Particularly, the most abundant metabolites, Pyrogallol-*O*-sulfate and Catechol-*O*-sulfate, had reached at 6 h a maximum concentration (C_{max}) of 11.4 µM and 12.2 µM, respectively (**Table 2.1**).

The identified (poly)phenol metabolites were then chemically synthetized[45]. Catechol-*O*-sulfate (Cat-sulf, 66% yield, pure) and Pyrogallol-*O*-sulfate (Pyr-sulf, 75% yield, mixture of two isomers in similar proportions) metabolites, synthetized as sodium salts, were selected for the present study. 100 mM stock solutions were prepared in dimethylsulfoxide (DMSO) (Fluka) and dilutions were performed in the cell culture medium described below, to final concentrations of 0.5 µM, 5 µM and 10 µM.

Table 2.1. Biochemical properties of the two most abundant human bioavailable (poly)phenol metabolites[52]. The corresponding nomenclature, abbreviation, chemical structure and maximum circulating concentrations (C_{max}) in human plasma[45] are presented.

Nomenclature	Abbreviation	Structure	C_{max} (µM)
Catechol-*O*-sulfate	**Cat-sulf**	HO⟷OSO$_3$H	**12.2 ± 5.9**
Pyrogallol-*O*-sulfate***	**Pyr-sulf**	OH / OSO$_3$H / OSO$_3$H / OH / OH / OH	**11.4 ± 6.7 (Pyr-2-sulf)** **0.65 ± 0.3 (Pyr-1-sulf)**

* The Pyrogallol-O-sulfate (Pyr-sulf) used in the present study consists of a mixture of two isomers in a similar proportion: 53% of Pyrogallol-2-*O*-sulfate (Pyr-2-sulf) and 47% of Pyrogallol-1-*O*-sulfate (Pyr-1-sulf). The C_{max} of each isomer was determined as they can be distinguished by chromatography.

2.2   N9 microglial cell culture

N9 cells, kindly provided by Dr. Teresa Pais (Instituto de Medicina Molecular, Universidade de Lisboa, Portugal), were cultured in a cell culture medium [Eagle Minimum Essential Medium (EMEM) supplemented with sodium bicarbonate (Sigma-Aldrich®), 200mM L-glutamine (Gibco®), 10% (v/v) heat inactivated fetal bovine serum (FBS) (Biowest) and a non-essential amino acid solution (NEAA) (Sigma-Aldrich®)]. Proper growth condition was ensured at 37 ˚C in a humified atmosphere, with 5% (v/v) of CO_2. Cellular growth was monitored under a microscope and regular changings of the culture

medium were performed, in order to reach an ideal confluence not higher than 70-80%[62]. The cellular maintenance was performed in T-flasks. For the subcultures, cells were detached from the bottom of the T-flasks by vigorous shaking without using detaching agents.

2.3 Detection of pro-inflammatory and anti-inflammatory mediators

To study the release of both pro-inflammatory and anti-inflammatory mediators in a neuroinflammatory model stimulated with LPS, microglia cells were cultured in 24-well plates or 6-well plates at a density of 2.5×10^5 cells.mL^{-1}.

The effect of human bioavailable (poly)phenol metabolites in the modulation of neuroinflammation was determined in a pretreatment approach. Different physiological concentrations of Cat-sulf and Pyr-sulf (0.5 µM, 5 µM or 10 µM) were added to cells and three different preincubation times were tested (2, 4 or 6 h). Afterwards, medium was discarded from each well and a fresh medium containing 300 ng.mL^{-1} of LPS from *Escherichia coli* 055:B5 (Sigma-Aldrich®, St. Louis, MO, USA) was administrated to cells as an insult at different time points. The release of mediators such as TNF-α, IL-10, IL-4, IL-1β and IL-6 were evaluated by ELISA (see 2.3.2 section), the NO by Griess reaction (see 2.3.1 section) and the intracellular superoxide levels by flow cytometry (see 2.3.3 section). In addition, the phosphorylation state of IκBα and NF-κB proteins was assessed by immunoblotting (see 2.3.4 section) and NF-κB nuclear translocation by immunocytochemistry (see 2.3.5 section).

2.3.1   Griess assay

Supernatants from cell cultures were collected from 24-well plates and stored at -80˚C until analysis. The release of NO was determined following 2, 4 and 6 h pretreatment with each (poly)phenol metabolite prior to the LPS stimulation for 24 h. NO production levels were assayed by Griess reaction, based on an indirect determination of nitrite (NO_2^-), a stable decomposition product of NO.

A standard curve (2 µM to 25 µM) was prepared with the previously described cellular medium, without any treatment or stimulation, containing a sodium nitrite solution ($NaNO_2$) (Sigma-Aldrich®) diluted 1:1000 in fresh medium. Then, 100 µL of each point of the standard curve, as well as samples, was added in triplicate to a 96-well plate. An equal volume of Griess Reagent (Sigma-Aldrich®, St. Louis, MO, USA) was added to the plate followed by incubation at room temperature for color development. The absorbance was recorded at 540 nm by Synergy HT microplate reader (Biotek®, Vermont, USA).

2.3.2   Enzyme-linked immunosorbent assay (ELISA)

Supernatants from cell cultures were collected from 24-well plates and stored at -80 ˚C until analysis. TNF-α release levels were determined following 2, 4 and 6 h pretreatment with each (poly)phenol metabolite prior to the LPS stimulation for 24 h. The other cytokine levels (IL-10, IL-4,

IL-1β and IL-6) were determined following 4 and 6 h pretreatment with Pyr-sulf prior to the LPS stimulation for 24 h. For all cytokines were performed an enzyme-linked immunosorbent assay (ELISA) in a sandwich format, using specific kits and according to manufacturers' instructions (PeproTech®; Princeton Business Park, Rocky Hill NJ, USA).

One specific plate for each cytokine was firstly coated with the antigen-specific capture antibody diluted in PBS. Then a blocking agent (1% (w/v) BSA in PBS) was added and incubated for 1h, preventing non-specific bindings. The standards and samples were added to the microplate in triplicates, incubated for 2 h. The standards, prepared in diluent (0.05% (v/v) Tween-20, 0.1% (w/v) BSA in PBS), were used for the calibration curve with defined concentrations of antigen. A second antibody, called detection antibody, was prepared in diluent prior to be added and incubated for 2 h, in order to detect specifically the antigen captured by the first antibody. The next step was the addition of the enzyme-linked avidin conjugate (1:2000 (v/v) in diluent) incubated for 30 min. Finally, 2,2'-azino-bis (3-ethylbenzothiazoline-6-sulphonic acid) (ABTS) liquid substrate was added to each well and the absorbance was measured at 405 nm with wavelength correction set at 650 nm using a Synergy HT microplate reader (Biotek®, Vermont, USA). Between each step of the method, all wells were systematically washed for four times, using 0.05% (v/v) Tween-20 in PBS solution. The standard curve was obtained by simple linear regression analysis of logarithmic transformed data obtained from titration of the reference standard. The samples data were then estimated from the standard curve.

2.3.3 Flow cytometry

N9 cells were cultured in 6-well plates and collected following a 4 h pretreatment with each (poly)phenol metabolite, prior to the LPS stimulation for 24 h. The production of superoxide ($O_2^{\bullet-}$) was quantified by flow cytometry.

The culture medium was removed from each well, cells were washed with PBS and detached from the bottom of the plates using 1mL FACS buffer (PBS with 2% FBS and 0.01% NaN$_3$). The content of each well was collected and spun down at 5000 g, and cells were washed once with FACS buffer. The staining step was performed by adding 5 µg.mL^{-1} DHE probe (Dihydroethidium, Invitrogen™, USA) that acts as an indicator of superoxide species. Events were acquired by CUBE 6 cytometer from Partec® and data were analyzed using the FlowJo software.

2.3.4 Protein extraction and quantification

N9 cells were cultured in 24-well plates and respective protein extracts were collected following a 6 h pretreatment with Pyr-sulf, prior to the LPS stimulation for 15 min, 30 min and 60 min.

Protein was extracted from cells with a lysis buffer consisting of a radioimmunoprecipitation solution (RIPA) [50 mM Tris pH 8 (CarlRoth®), 150mM NaCl (Panreac Applichem), 0.1% (w/v) sodium dodecyl sulfate (SDS) (Merk Milipore), 1% (v/v) nonylphenyl polyethylene glycol (NP-40)

(Calbiochem), 0.05% (w/v) sodium deoxycholic acid (Sigma-Aldrich®), protease and phosphatase inhibitors (Roche, Mannheim, Germany)]. The protein fraction was obtained by a centrifugation step at 13000 g for 10 min at 4 ˚C and stored at -80 ˚C until analysis. For protein quantification, a standard curve was prepared from serial dilutions of bovine serum albumin (BSA) (Sigma-Aldrich®) and the protein levels in each fraction were then estimated. All samples were added in triplicate to a 96-well plate. Protein content was measured by adding the Bradford reagent to each well (Quick Start™ Bradford 1x Dye Reagent, BioRad®) and Abs_{595} were recorded by Synergy HT microplate reader.

2.3.5   Western Blotting (Immunoblotting)

Immunoblotting assays were carried out for the analysis of IκBα and NF-κB protein and phosphorylation levels. 30 μg of total protein were mixed with sample buffer [0.24 M Tris pH 6.8 (CarlRoth®), 18% (v/v) β-Mercaptoetanol (Sigma-Aldrich®), 8% (w/v) SDS (Merk Milipore), 40% (v/v) Glycerol (Sigma-Aldrich®) and 0.1% (w/v) Bromophenol Blue (Sigma-Aldrich®)] and the mixtures were boiled at 100 ˚C for 5 min. Proteins were resolved by SDS-PAGE in 12% and 4% (w/v) acrylamide for resolving and stacking gels, respectively. Proteins were transferred to polyvinylidene difluoride (PVDF) membranes (BioRad®, USA) during 7 min at 200 Volts (V) and the membranes were blocked either with 5% (w/v) non-fat milk or 5% (w/v) MBA (membrane blocking agent) (GE Healthcare™, Buckinghamshire, UK) in Tris-Buffered Saline-Tween 20 (TBST) [50 mM Tris pH 7.6, 150 mM NaCl, 0.05% (v/v) Tween 20] for 1 h with agitation at room temperature (RT). Membranes were incubated overnight at 4 ˚C with the following primary antibodies: phospho-IκBα(Ser32/36) (1:500; Ref. #9246), phospho-NF-κB p65(Ser536) (1:500; Ref #3033) (Cell Signaling Technology), IκBα (1:200; Ref. sc-371), NF-κB p65 (1:300; Ref. sc-372) (Santa Cruz Biotechnology), and the loading control glyceraldehyde 3-phosphate dehydrogenase (GAPDH) (1:5000; Ref #MA5-15738) (Thermo Scientific, Canada). After washing the membranes three times with TBST for 5 min, the membranes were incubated for 2 h with agitation at RT with the following secondary antibodies, as required: goat anti-rabbit IgG peroxidase conjugated (1:5000; Ref #A6154) (Sigma-Aldrich®, USA) or goat anti-mouse IgG peroxidase conjugated (1:5000; Ref #31430) (Pierce, Thermo Scientific, USA). The membranes were washed 3 times with TBST for 5 min and protein signals were detected by the addition of enhanced chemiluminescence (ECL) substrate (GE Healthcare™, UK). The proteins of interest were visualized and analyzed using the Molecular imager ChemiDoc XRS (Quantity One™ software v.4.6.6; BioRad®, Portugal).

2.3.6   Immunocytochemistry

To assess the translocation of the NF-κB protein into the nucleus, microglia cells were cultured in 24-well plates, containing coverslips, and collected following 2, 4 and 6 h pretreatment with Pyr-sulf prior to the LPS stimulation for 15 min, 30 min and 60 min.

Culture medium was discarded and cells were treated with a fixation agent, Paraformaldehyde (PFA) [pH 7.2, PFA 4% (v/v), sucrose 4% in phosphate buffer saline (PBS)]. The permeabilization and blocking steps were performed by adding a solution containing Triton 0.1%(v/v) (Sigma-Aldrich®) in PBS and BSA 3% (w/v) (Sigma-Aldrich®) in PBS for 20 min at RT. Coverslips were then incubated with NF-κB p65 (1:200; Ref. sc-372) (Santa Cruz Biotechnology) as the primary antibody, diluted in the Triton-PBS-BSA solution for 2 h at RT. After washing coverslips three times with PBS, the secondary antibody, goat anti-rabbit AlexaFluor 594 (1:500; Ref #A11037) (Sigma-Aldrich®, USA) diluted in PBS, was added and incubated for 1 h at RT. One drop of Prolong Gold (Invitrogen, USA) was added to each coverslip, mounted in glass slides and stored at 4 °C overnight until microscope image acquisition. Images were acquired using a Leica DM6 B (Leica Application Suitex, software version 1.90.13747) widefield microscope equipped with a cooled CCD camera (Roper Scientific Coolsnap HQ). Total of 1128 photos from different fields were collected, with a mean of 30 cells, comprising all the conditions and the respective biological replicates (at least three). Data were assessed by counting the total number of cells and those with nuclear distribution of NF-κB, using the ImageJ software (NIH, USA). NF-κB translocation was estimated as the ratio between cells with nuclear NF-κB and the total number of cells.

2.3.7 Statistical analysis

In this study, data are represented as the mean ± standard error of the mean (SEM) of three independent experiments. Statistical significance was assessed using one-way ANOVA with Sidak's multiple comparison or t-tests with Mann-Whitney test, considering $p\text{-value} < 0.05$ as significant differences. In all figures, statistical significances are indicated as $*p < 0.05$, $**p < 0.01$ and $***p < 0.001$.

3.   RESULTS AND DISCUSSION

Previous work from the *Molecular Nutrition and Health Laboratory* has shown a protective effect of two human bioavailable and BBB permeable (poly)phenol metabolites (Pyr-sulf and Cat-sulf) in a cell model of neuroinflammation[52]. The model consisted of a LPS-stimulated N9 microglial cell line, to which 300 ng.mL^{-1} of LPS was added for 24 h to activate microglial cells. The protective effect was observed following a preincubation of microglia cells with 5 µM of each (poly)phenol metabolite for 6 h prior to the LPS insult[52]. In the present study, the concentrations of both metabolites used were based upon a previous human intervention study, where their circulating levels were determined[45].The calculated averages of the maximum concentrations in plasma samples (C_{max}) were 11.4 µM and 12.2 µM at 6 h for Pyr-sulf and Cat-sulf, respectively. It should be noted that in some volunteers these metabolites reached maximum plasma concentrations of around 20 µM[45]. In that same human intervention study, the period of time during which Pyr-sulf and Cat-sulf circulate was found to be between 2 and 6 h[45].

Based upon these parameters, one of the aims of the present study was to test, in the same cell model of neuroinflammation, the efficacy of Pyr-sulf and Cat-sulf at lower concentrations than previously studied and for periods of time within their time of circulation in the human plasma.

3.1   The influence of (poly)phenol metabolite dose and incubation time on neuroinflammatory mediators

The modulation of a microglial inflammatory state, following a preincubation with Pyr-sulf or Cat-sulf metabolites, was analyzed by looking for a set of specific cellular mediators. Final concentrations of 0.5 µM, 5 µM and 10 µM of both metabolites, incubated with cells for 2, 4 and 6 h prior to a 24 h LPS stimulation, represent the experimentally tested conditions.

NO and TNF-α are two of the most studied and well-known cellular mediators released in response to a LPS inflammatory stimulus and are described as general markers of a pro-inflammatory response. Both mediators were evaluated in order to follow the microglial cellular response to a LPS stimulus, with and without a preincubation with (poly)phenol metabolites.

With respect to NO levels, no significant modulation of NO levels was observed in response to Pyr-Sulf (**Figure 3.1B**). Significant differences were only observed for Cat-sulf, which appears to increase the inflammatory process following a 2 h preincubation at a final concentration of 0.5 µM (**Figure 3.1A**). However, the same concentration of Cat-sulf was shown to result in a significant decrease in NO levels following a 6 h preincubation. (**Figure 3.1A**). This modulation effect was not observed for other Cat-sulf concentrations (**Figure 3.1A**). It led us to suggest that Cat-sulf, at lower concentrations, may have the ability to influence the release of NO. Initially promoting an increase (2 h preincubation), but eventually resulting in a reduction in the levels of NO following a 6 h preincubation and 24 h LPS insult. Despite the fact that NO levels do not represent the most robust indicator of an

inflammatory state, this result is very interesting and suggests that lower levels of Cat-sulf in circulation could exert an attenuating effect on the release of NO.

For the same cell model, the effect of both metabolites on the release of NO was previously described for a concentration of 5 µM and for a preincubation time of 6 h. Under these conditions, no effect on levels of released NO was observed[52]. The fact we may have effects at both at lower concentrations and during shorter preincubation times (than previously investigated) reinforces the potential of these metabolites under physiologically relevant conditions.

A

LPS (300 ng.mL^{-1})	+	+	+	+	+	+	+	+	+	+	+	+
Cat-sulf (µM)	-	0.5	5	10	-	0.5	5	10	-	0.5	5	10
Time of incubation		2 h				4 h				6 h		

B

LPS (300 ng.mL^{-1})	+	+	+	+	+	+	+	+	+	+	+	+
Pyr-sulf (µM)	-	0.5	5	10	-	0.5	5	10	-	0.5	5	10
Time of incubation		2 h				4 h				6 h		

Figure 3.1. Effects of (poly)phenol metabolites on NO levels in N9 murine microglial cells stimulated with LPS. Pretreatments with (poly)phenol metabolites were performed with the indicated concentrations for 2, 4 and 6 h, followed by a LPS stimulation (300 ng.mL^{-1}) for 24 h. **(A)** Microglial cells treated with Catechol-sulfate (Cat-sulf) at the indicated concentrations; **(B)** Microglial cells treated with Pyrogallol-sulfate (Pyr-sulf) at the indicated concentrations. Both quantifications were performed by a Griess reaction and the results normalized for LPS control values. Black solid bars represent cells that were subjected to a LPS stimulation without any (poly)phenol pretreatment (positive control); Grey solid bars and white dotted bars represent cells subjected to (poly)phenol pretreatment followed by LPS stimulation. Data represent mean ± standard error of the mean (SEM) of three independent biological replicates; Statistical differences are relative to LPS incubation (positive control), for each time point and pretreatment, denoted as * p<0.05.

Levels of secreted TNF-α were also assessed under the same experimental conditions. Preincubation with Cat-sulf led to a significant decrease in TNF-α levels, observed following 4 and 6 h incubations with this metabolite at concentrations of 5 µM and 10 µM (**Figure 3.2A**). The strongest effect on cytokine release occurred following 6 h of preincubation (**Figure 3.2A**). Two hours of preincubation with Cat-sulf did not show any modulatory effect. (**Figure 3.2A**).

The greatest reduction in TNF-α levels was observed following Pyr-sulf preincubation. All tested concentrations of this metabolite were revealed to be effective. The greatest attenuation of TNF-α levels was observed following a 4 h preincubation with 0.5 µM Pyr-sulf compared with LPS alone condition (**Figure 3.2B**). However, there is no difference between that condition and a 6 h preincubation with 5 µM and 10 µM Pyr-sulf. In contrast, a different behavior was observed for a 2 h preincubation with 10 µM of Pyr-sulf: TNF-α levels increased significantly in comparison with cells that were not pretreated prior to LPS stimulation (**Figure 3.2B**). It should be noted that Pyr-sulf incubation *per se* did not affect the production of TNF-α at both 4 and 6 h of incubation (data not shown). But, a 2 h incubation with Pyr-sulf alone did induce a very slight increase in TNF-α levels (**Figure 3.3**).

Previous research using the same cell model was performed in order to evaluate the effect of a pretreatment with both metabolites (5 µM for 6 h) on TNF-α levels[52]. No modulatory effect was observed following Cat-sulf pretreatment. Preincubation with Pyr-sulf resulted in a stronger attenuation effect on TNF-α levels. In addition, the same study gave new insights into the endothelium transport of bioavailable (poly)phenol metabolites. Pyr-sulf was transported across the BBB in small quantities (approximately 5% with 2 h of incubation)[52]. The fact that we observe a powerful effect of Pyr-sulf preincubation on TNF-α levels, even at very low concentrations, is encouraging. These are likely to be representative of the physiological concentrations that will reach the brain.

A

LPS (300 ng.mL^{-1})	+	+	+	+	+	+	+	+	+	+	+	+
Cat-sulf (μM)	-	0.5	5	10	-	0.5	5	10	-	0.5	5	10
Time of incubation		2 h				4 h				6 h		

B

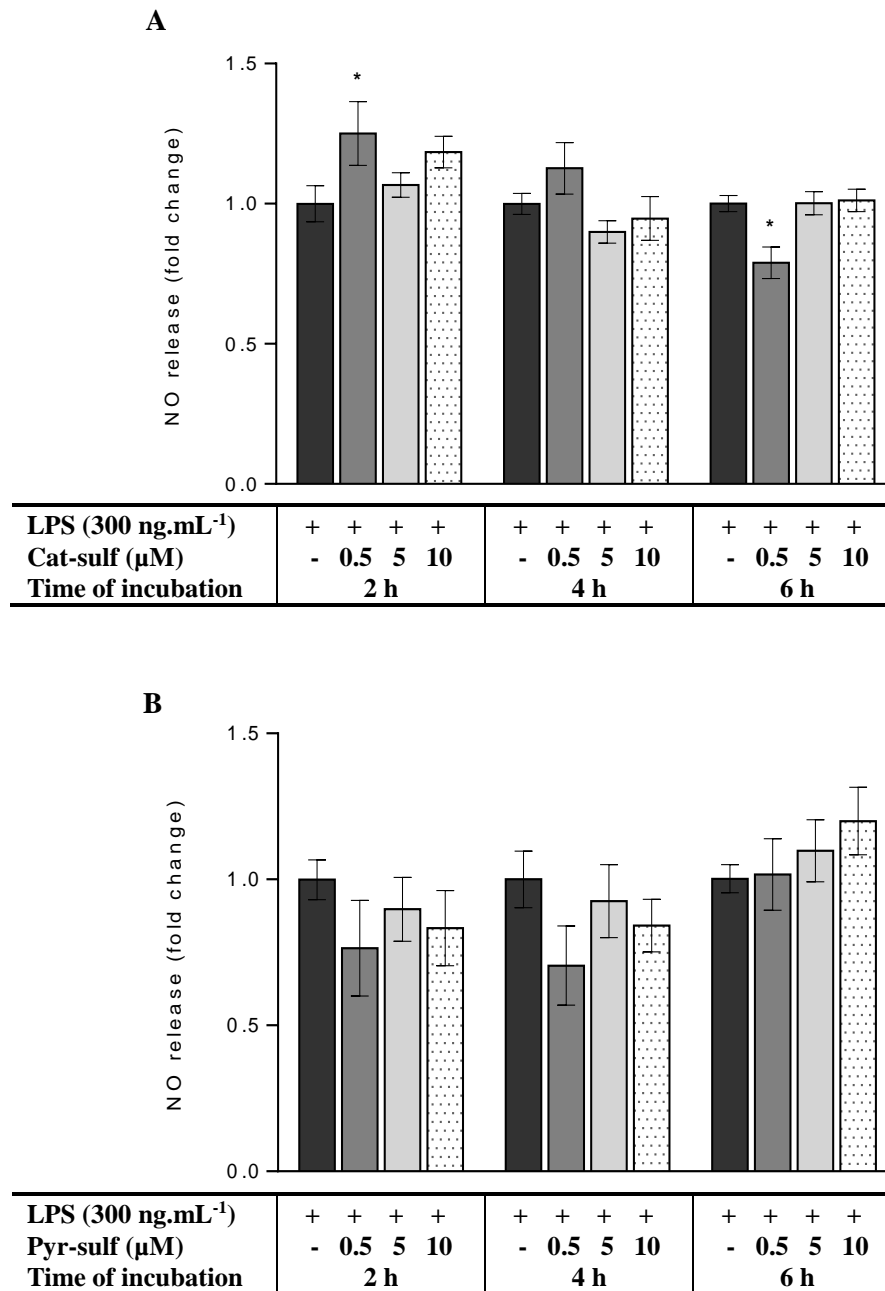| LPS (300 ng.mL^{-1}) | + | + | + | + | + | + | + | + | + | + | + | + |
| Pyr-sulf (μM) | - | 0.5 | 5 | 10 | - | 0.5 | 5 | 10 | - | 0.5 | 5 | 10 |
| Time of incubation | | 2 h | | | | 4 h | | | | 6 h | | |
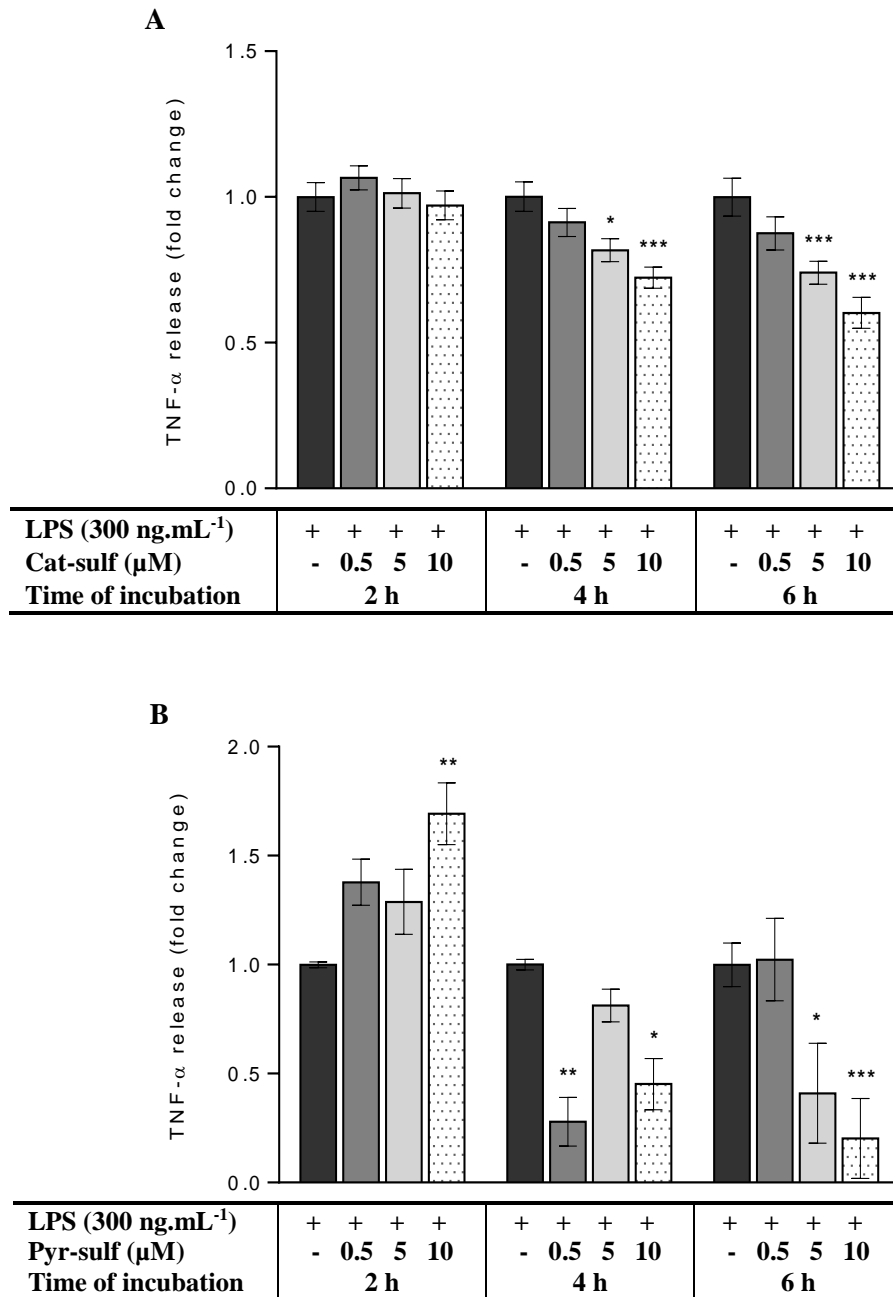
Figure 3.2. Effects of (poly)phenol metabolites on TNF-α levels in N9 murine microglial cells stimulated with LPS. Pretreatments with (poly)phenol metabolites were performed with the indicated concentrations for 2, 4 and 6 h, followed by a LPS stimulation (300 ng.mL^{-1}) for 24 h. **(A)** Microglial cells treated with Catechol-sulfate (Cat-sulf) at the indicated concentrations; **(B)** Microglial cells treated with Pyrogallol-sulfate (Pyr-sulf) at the indicated concentrations. Both quantifications were performed by an ELISA method and the results normalized for LPS control values. Black solid bars represent cells only subjected to a LPS stimulation without any (poly)phenol pretreatment (positive control); Grey solid bars and white dotted bars represent cells subjected to (poly)phenol pretreatment followed by LPS stimulation. Data represent mean ± standard error of the mean (SEM) of three independent biological replicates; Statistical differences are relative to LPS incubation (positive control), for each time point and pretreatment, denoted as ***p<0.001, **p<0.01 and *p<0.05.
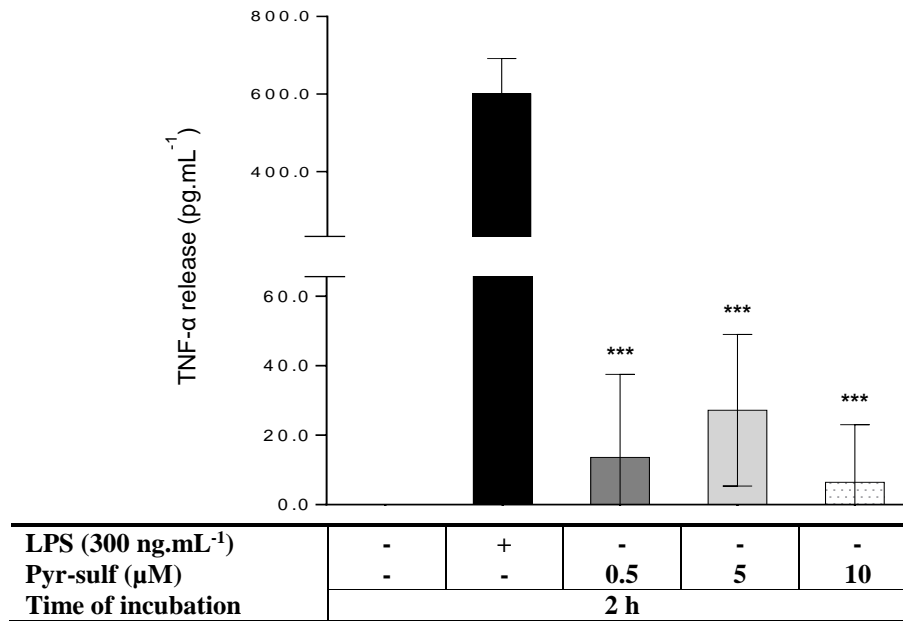
Figure 3.3. Effects of Pyrogallol-sulfate (Pyr-sulf) on TNF-α levels in N9 murine microglial cells. Microglial cells were treated with the indicated concentrations for 2h. Quantifications were performed using an ELISA methodology. The black solid bar represents cells that were only subjected to a LPS stimulation without any pretreatment with (poly)phenol metabolites (positive control); The grey solid bar and the white dotted bar represent cells subjected to a (poly)phenol treatment only (no subsequent LPS stimulation). Data represent mean ± standard error of the mean (SEM) of three independent biological replicates; Statistical differences are relative to LPS incubation (positive control) and are denoted as ***p<0.001.

Overall, it is clear that following a 2 h preincubation with Pyr-sulf or Cat-sulf we did not detect a decrease in the levels of either TNF-α or NO inflammatory mediators. A reduction in TNF-α levels was only observed following preincubations of 4 and 6 h (with Pyr-sulf and Cat-sulf). Between the two, Pyr-sulf appeared to be the most promising metabolite, since it promoted a marked reduction in TNF-α levels even at low concentrations (0.5 µM). Therefore, we focused the study on other inflammatory mediators of this metabolite for incubation times of 4 and 6 h.

Besides TNF-α and NO, there are other pro-inflammatory mediators involved in the microglial response, namely IL-1β[63] and IL-6[64]. Both cytokines were evaluated using commercially available ELISA kits. Detection of IL-1β and IL-6 was not achieved for any of the tested conditions using the aforementioned kits (section 2.3.2).

Previous studies have investigated whether the release of the IL-1β cytokine by microglia cells plays an active role in brain tissue towards an endotoxin injury. It was described that for IL-1β release, a second inflammatory stimulus is required, since a single endotoxin stimulation is inefficient[65]. In contrast, alternative studies using the same cells reported the detection of significant IL-1β levels following a single LPS stimulation[66]. Despite these reported incongruities, we decided to analyze IL-1β cytokine levels released by N9 murine microglia cells in response to a single LPS stimulus. After being

unable to detect IL-1β in our samples, we hypothesized that a single LPS treatment, in fact, may not be sufficient to stimulate this cytokine to detectable levels. To test this, one possibility is to try a combined stimulation using both LPS and ATP. A combined LPS and ATP stimulation has been described to induce IL-1β secretion from microglial cells[65]. In other studies performed using N9 microglia cells, a stimulation with only LPS did not result in levels of the mature form of IL-1β that could be detected by western blot, and of the total levels of IL-1β by ELISA assay[67]. However the conditions tested by these authors were different from the ones in the present study: LPS stimulation was carried out at a concentration of 100ng.mL^{-1} for 6 h and a higher cell density was also used (10^6 cells.mL^{-1}). In other studies also using the N9 microglial cell line, significant levels of IL-1β were observed following a stimulation with 1000 ng.mL^{-1} of LPS for 24 h, and at a cell density in a comparable range to the present study (10^5 cells.mL^{-1})[68,69]. Therefore, we may explain the absence of detectable IL-1β under our conditions, as being due to the lower concentration of LPS used. If higher concentrations of LPS had been tested for the same period of time (24 h), the IL-1β cytokine might have reached detectable levels.

The inability to detect IL-6 in our experiments was unexpected. In a study performed with the N9 microglial cell line, at a similar cell density to the one used in our work (10^5 cells.mL^{-1}) but with a higher concentration of LPS (1000 ng.mL^{-1}), an IL-6 cytokine increase was observed following a 24 h stimulation[68,69,70]. The difference in the LPS concentration could explain our inability to detect IL-6 in our experiments. Furthermore, technical difficulties in establishing an IL-6 standard curve using the commercial assay kit chosen greatly hampered this section of the work.

Concerning the modulation of TNF-α levels following Pyr-sulf pretreatment, mainly: (i) the slight increase in TNF-α levels promoted by Pyr-sulf *per se* at 2 hours of incubation; (ii) the pro-inflammatory effect after 2h of preincubation followed by a LPS treatment; and (iii) that this pro-inflammatory effect did not prevail at later time points, we hypothesize a mild inflammatory preconditioning role of Pyr-sulf. Under this situation, we expect that this mild inflammatory stimulus could improve the cellular response to a greater subsequent inflammatory insult.

Regarding the exposure of microglia to an initial inflammatory insult, a lag period between an early pro-inflammatory response and a later anti-inflammatory microglial response is described. This transition culminates in restored cellular homeostasis[6]. Thus, we also looked at some anti-inflammatory cytokines, following 4 and 6 h of Pyr-sulf preincubation. IL-4 and IL-10 levels were assessed in order to evaluate the ability of Pyr-sulf to elicit an anti-inflammatory response in the microglia naïve cells. However, levels of both cytokines were below the sensitivity of the commercial ELISA kit used (data not shown). These results suggested that the protective capacity of the Pyr-sulf metabolite, observed following LPS treatment, may not be related to a preconditioning effect triggered by an anti-inflammatory microglial response, at least not a response mediated by IL-4 and IL-10 cytokines at the time points investigated. Instead, other cellular mechanisms may be acting to modulate the microglia cells' immune response to this preconditioning effect.

Besides the aforementioned cytokines and NO mediator, other molecular players could be followed as markers of microglial activation. Superoxide ($O_2^{\bullet-}$) is described as being produced by microglia in response to different cellular stimuli, amplifying the microglial pro-inflammatory function[71,72]. To assess the production of intracellular levels of $O_2^{\bullet-}$, N9 microglia cells were preincubated with both Cat-sulf and Pyr-sulf for 4h and then stimulated with LPS for 24 h, prior to being stained with a specific probe, dihydroethidium (DHE). A flow cytometry assay was performed as described in the methods section (section 2.3.3). Unfortunately, during the assay some technical issues occurred with the flow cytometer, hampering the collection of all experimental replicates, including the positive control with hydrogen peroxide. The equipment was out of order for the remaining time of the thesis experimental work and therefore we were not able to proceed with the analysis of all necessary biological replicates. Nevertheless, for the samples acquired a trend is observed following treatment with Pyr-sulf and Cat-sulf. This data is included for illustrative purposes.

As expected, an increase in $O_2^{\bullet-}$ levels was observed following LPS stimulation (**Figure 3.4** and **Figure 3.5**), observed both by an increase in the number of DHE positive cells (**Figure 3.4A** and **Figure 3.5A**) and by a shift in the median fluorescence intensity (DHE fluorescence; **Figure 3.4B** and **Figure 3.5B**). Regarding the pretreatment with Cat-sulf, we were able to see that the percentage of DHE positive cells for the lowest concentration tested (0.5 µM) was reduced when compared to the LPS stimulation alone, resembling the naïve cells **(Figure 3.4A)**. The ability of Cat-sulf to decrease the percentage of cells producing $O_2^{\bullet-}$ decreases with increasing concentrations of this metabolite (**Figure 3.4A**). However, all cells naturally produce $O_2^{\bullet-}$ at a basal level[73]. Thus, it was also important to observe the intensity of the fluorescence emitted by the cells (**Figure 3.4B**). Despite the fact that pretreatment with 10 µM Cat-sulf results in the highest percentage of cells with increased production of $O_2^{\bullet-}$ (**Figure 3.4A**), this metabolite shows the lowest levels of MFI when compared to cells only stimulated with LPS (**Figure 3.4B**). On the other hand, the most heterogeneous population (a wider spread with possibly two peaks – suggesting the existence of two subpopulations of cells) was observed at 0.5 µM and 5 µM Cat-sulf (**Figure 3.4B**).

A

B
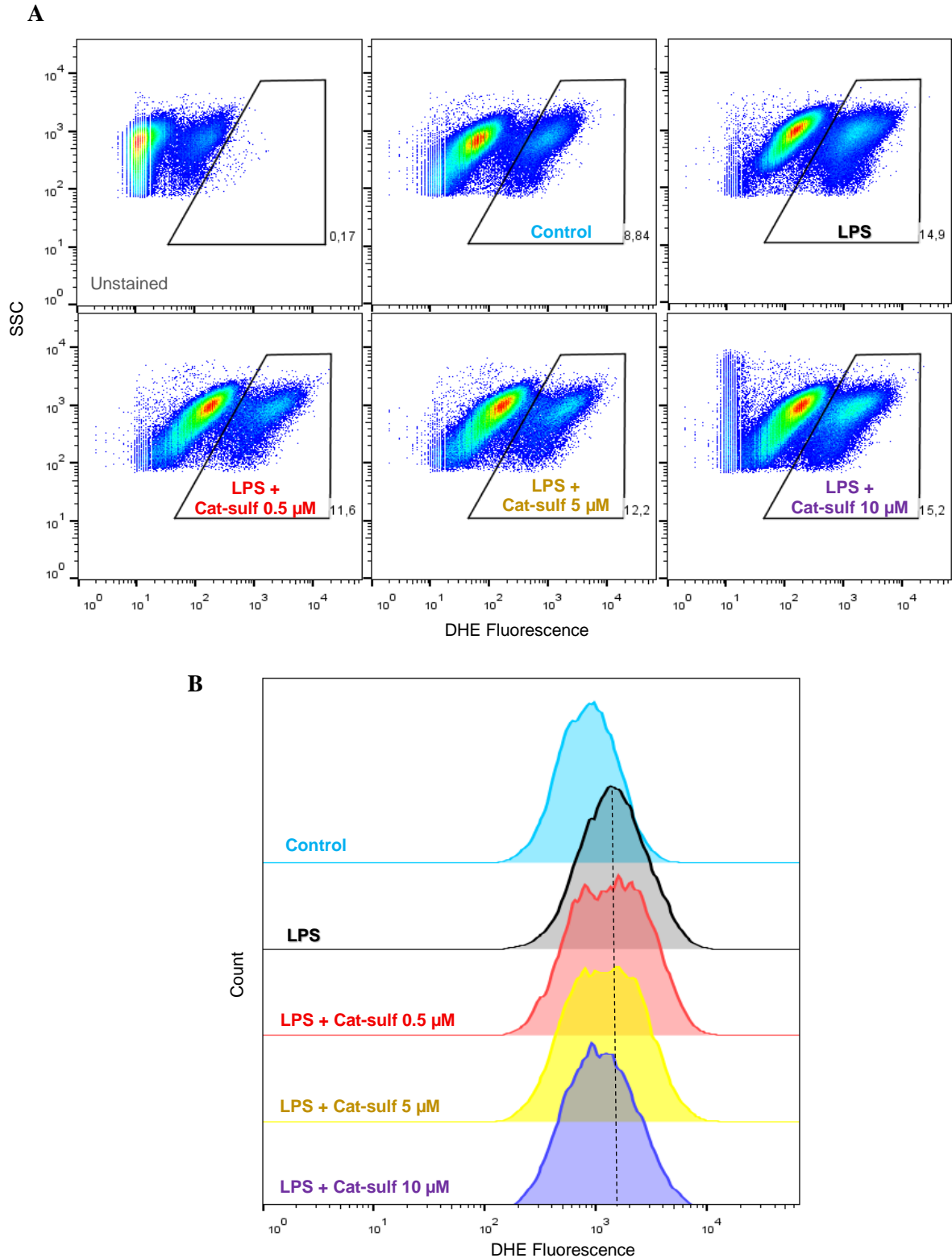
Figure 3.4. Production of intracellular superoxide ($O_2^{\bullet-}$) by N9 murine microglial cells in the presence of the Catechol-sulfate (Cat-sulf) (poly)phenol metabolite. Pretreatments with Cat-sulf were performed with the indicated concentrations for 4 h prior to being stimulated with LPS (300 ng.mL^{-1}) for 24 h. Superoxide levels were assessed by flow cytometry and the results analyzed using FlowJo software. **(A)** DHE positive cells represented in the selected section by the superoxide radical fluorescence using the DHE probe versus the side scatter (SSC) signal intensity of the cells. **(B)** Histogram of number of cells (normalized) versus DHE fluorescence intensity of the section selected in **A**. Vertical dashed line is pointing MFI at the peak of LPS condition. Data represent only one sample.

Concerning Pyr-sulf preincubation, a different behavior was observed in relation to the levels of $O_2^{\cdot-}$ produced. The metabolite concentration that exhibited the lowest percentage of DHE positive cells was 10 µM (**Figure 3.5A**). In contrast, the lowest concentration of Pyr-sulf (0.5 µM) exhibited the highest percentage of DHE positive cells. With regard to the MFI, preincubation with Pyr-sulf resulted in the appearance of heterogeneous peaks, suggesting once more the existence of different populations compared to the naïve cells (control) and the LPS only condition (**Figure 3.5B**). However, there are no clear differences between the Pyr-sulf pretreatment conditions in the MFI (**Figure 3.5B**).

Overall, from the analysis of the effect of Cat-sulf and Pyr-sulf on the intracellular superoxide levels produced by microglia cells, Cat-sulf most efficiently reduced the MFI of intracellular $O_2^{\cdot-}$ at 10 µM and the percentage of DHE positive cells at 0.5 µM. On the other hand, for Pyr-sulf no reduction effect on the MFI levels was observed for the tested concentrations, and these levels were even slightly higher than the LPS alone condition.

As previously stated: there were technical difficulties with this section of work. Further confirmation is required; the necessary experimental replicates should be performed.

It is important to note that a previous study in this cell model described the effect of both of these metabolites on the production of the intracellular superoxide. Pyr-sulf and Cat-sulf were both tested at a concentration of 5 µM with a preincubation time of 6 h prior to stimulation with LPS for 24 h. Pretreatment was not observed to have any effect[52].
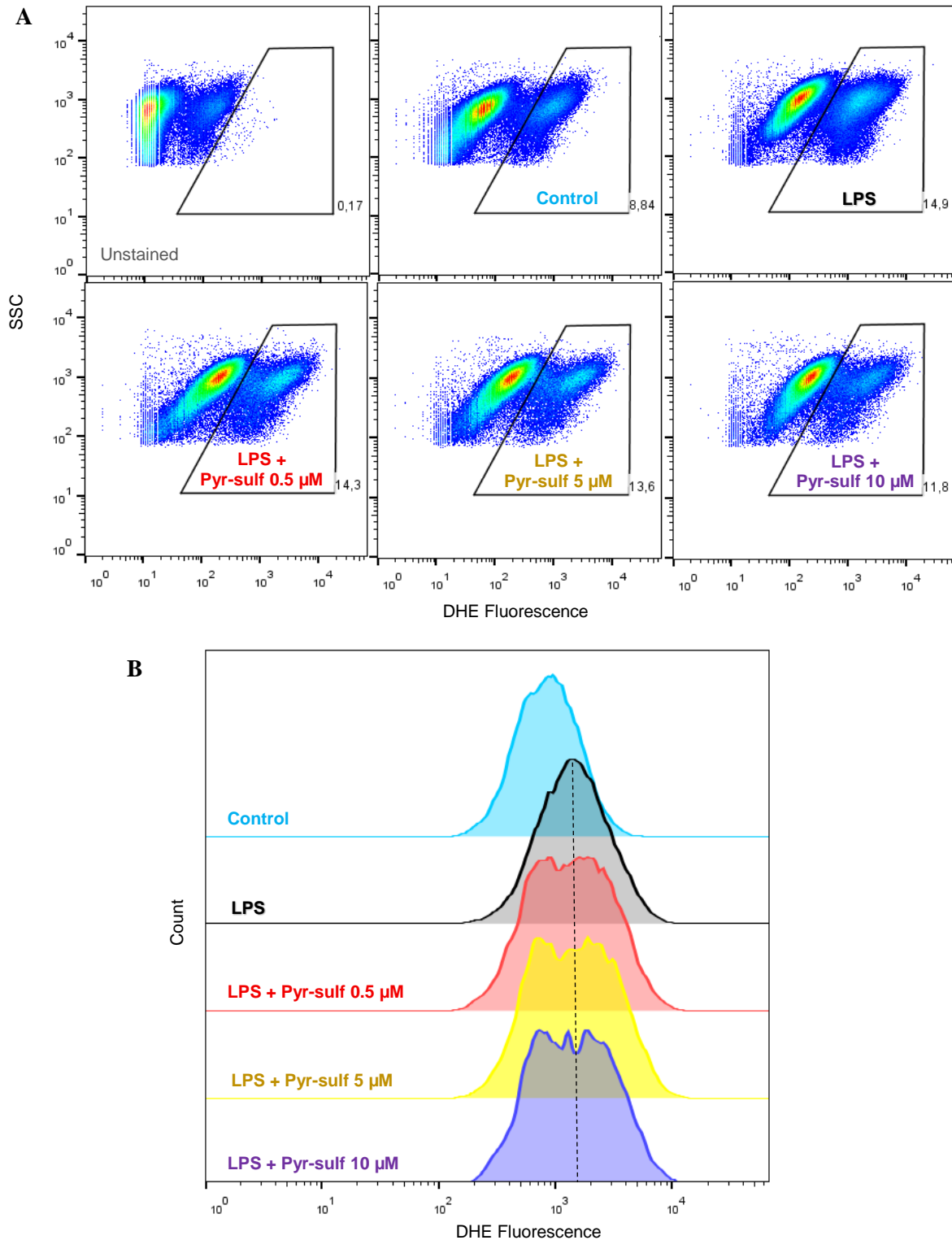
Figure 3.5. Production of intracellular superoxide ($O_2^{\cdot-}$) by N9 murine microglial cells in the presence of the Pyrogallol-sulfate (Pyr-sulf) (poly)phenol metabolite. Pretreatments with Pyr-sulf were performed with the indicated concentrations for 4 h prior to LPS stimulation (300ng.mL^{-1}) for 24 h. Superoxide levels were assessed by flow cytometry and the results analyzed using FlowJo software. **(A)** DHE positive cells represented in the selected section by the superoxide radical fluorescence using the DHE probe versus the side scatter (SSC) signal intensity of the cells. **(B)** Histogram of number of cells (normalized) versus DHE fluorescence intensity of the section selected in **A**. Vertical dashed line is pointing MFI at the peak of LPS condition. Data represent only one sample.

3.2   Modulation of NF-κB signaling pathway by Pyrogallol-sulfate

Most of the inflammatory mediators discussed up to this point (e.g cytokines) are included on an extensive list of targets that are highly regulated by the NF-κB transcription factor[21]. Thus, it was imperative to study this signaling pathway by looking for pathway-specific markers. To understand the extent to which the NF-κB pathway may be affected by Pyr-sulf, the N9 microglial cell line was preincubated with this metabolite prior an LPS stimulation. NF-κB total protein levels and the phosphorylation state of NF-κB p65 and the IκBα inhibitor were evaluated. Additionally, NF-κB p65 nuclear translocation was also analyzed.

Previous work from the *Molecular Nutrition and Health Laboratory* revealed that Pyr-sulf pretreated cells displayed a reduced translocation of NF-κB to the nucleus following 60min of LPS stimulation, concomitant with the modulation of IκBα protein levels[52]. In order to further build upon this early work, the same experimental conditions were also used in this current study: cellular pretreatment with 5 μM of Pyr-sulf for 6 h, followed by different LPS exposure times (0, 15, 30 and 60 min).

Under normal conditions, NF-κB is retained in the cytoplasm, in an inactivated form. This retention is under the control of the IκBα inhibitory protein. Thus, we began our analysis by studying this NF-κB negative regulator. IκBα total protein levels exhibited a significant decrease 30 min after the LPS stimulation in microglia cells (no pretreatment) compared with non-stimulated cells (**Figure 3.6**). However, the same reduction was noticed following pretreatment with Pyr-sulf. This trend was reversed 60 min after the LPS addition, with the pretreated cells showing a larger increase in IκBα total protein levels (though not significantly larger; **Figure 3.6**). In addition, Pyr-sulf by itself, without any LPS stimulation, appears to increase the basal level of IκBα when compared to the untreated cells. (**Figure 3.6**).
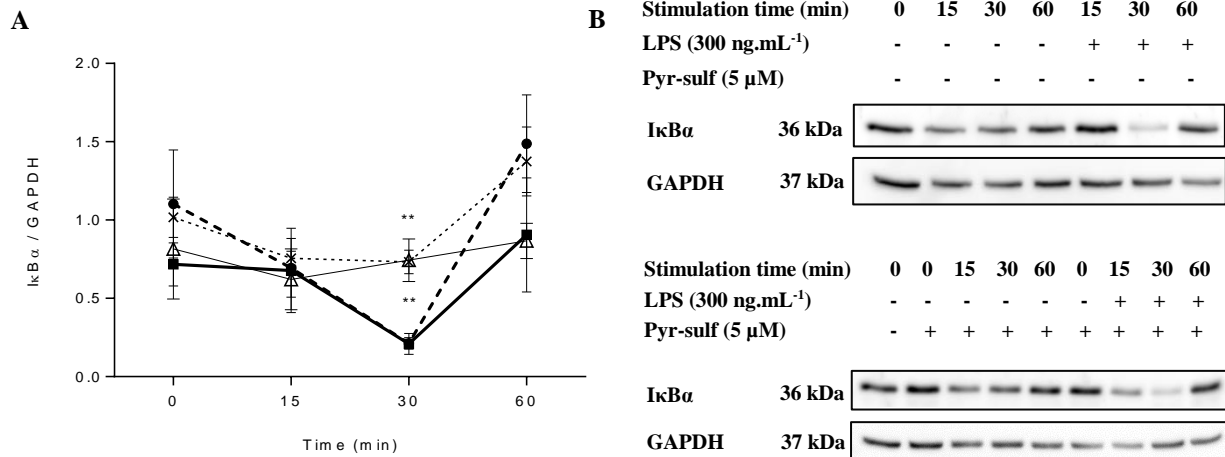
Figure 3.6. Modulation of IκBα protein levels by Pyrogallol-sulfate (Pyr-sulf) metabolite in N9 murine microglial cells stimulated with LPS. Pretreatment with Pyr-sulf was performed using a concentration of 5 μM for 6 h prior to the stimulation with LPS (300 ng.mL^{-1}) for different incubation times, 0, 15, 30 and 60 min. **(A)** Time course of the IκBα total protein levels and **(B)** representative western blots of IκBα total protein using GAPDH as a loading control. Black solid line with white triangles represents naïve cells without any treatment (pretreatment or LPS stimulation; negative control); Dotted line with cross symbols represents cells only treated with Pyr-sulf (positive control for metabolite); Bold solid line with squares represents LPS-stimulated cells (positive control for stimulus); Dashed line with solid circles represents cells pretreated with Pyr-sulf and then stimulated with LPS. Data represent mean ± standard error of the mean (SEM) of three independent biological replicates; Statistical differences are relative to LPS control, for each time point and pretreatment, denoted as **p<0.01.

To determine the effects of Pyr-sulf on the phosphorylation status of IκBα, the ratio of IκBα phosphorylated protein to IκBα total protein was assessed. As expected, an increase of IκBα phosphorylation was observed in the presence of LPS (**Figure 3.7**). This is known to be linked to a subsequent proteasomal degradation and to the release of active NF-κB from IκBα inhibition. Interestingly, pretreatment with Pyr-sulf metabolite modulated IκBα phosphorylation, following LPS stimulation, and the greatest effect was seen at 60 min (**Figure 3.7**). The remarkable effect of Pyr-sulf on this NF-κB inhibitory protein suggests that it possesses the ability to attenuate one of the main regulatory steps of the NF-κB inflammatory cascade.
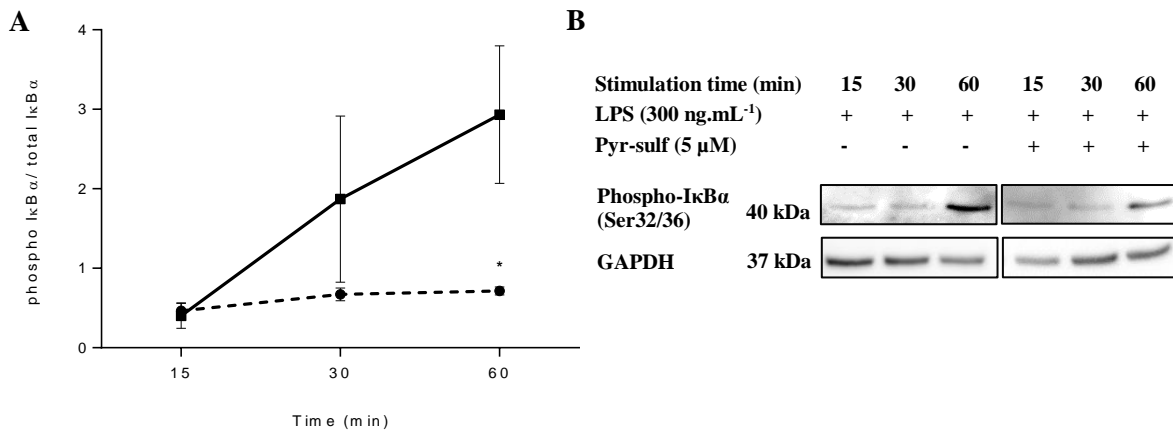
Figure 3.7. Kinetics of IκBα phosphorylation in the presence of Pyrogallol-sulfate (Pyr-sulf) metabolite in N9 murine microglial cells stimulated with LPS. Pretreatment with Pyr-sulf was performed using a concentration of 5 μM for 6 h prior to the stimulation with LPS (300ng.mL^{-1}) for different incubation times 15, 30 and 60 min. **(A)** IκBα phosphorylation (at Ser32/36) ratio with time and **(B)** representative western blots of IκBα phosphorylated state using GAPDH as a loading control. Black solid line represents cells only stimulated with LPS (control); Dashed line represents cells pretreated with Pyr-sulf prior to LPS stimulation. Data represent mean ± standard error of the mean (SEM) of three independent biological replicates; Statistical differences are relative to LPS control, for each time point, denoted as *p<0.05.

To complement this work, total and phosphorylated levels of NF-κB and its nuclear translocation were analyzed. Regarding total protein levels of NF-κB, no significant differences were found between conditions (**Figure 3.8**). The incubation of microglia cells with Pyr-sulf presented the highest NF-κB protein levels, cells treated with LPS only remained almost unchanged with time (**Figure 3.8**).

A

B

Stimulation time (min)	15	30	60	0	15	30	60
LPS (300 ng.mL^{-1})	-	-	-	-	+	+	+
Pyr-sulf (5 µM)	-	-	-	-	-	-	-

NF-κB p65   64 kDa

GAPDH   37 kDa

| Stimulation time (min)	0	15	30	60	0	15	30	60
LPS (300 ng.mL^{-1})	-	-	-	-	-	+	+	+
Pyr-sulf (5 µM)	-	+	+	+	+	+	+	+

NF-κB p65   64 kDa

GAPDH   37 kDa
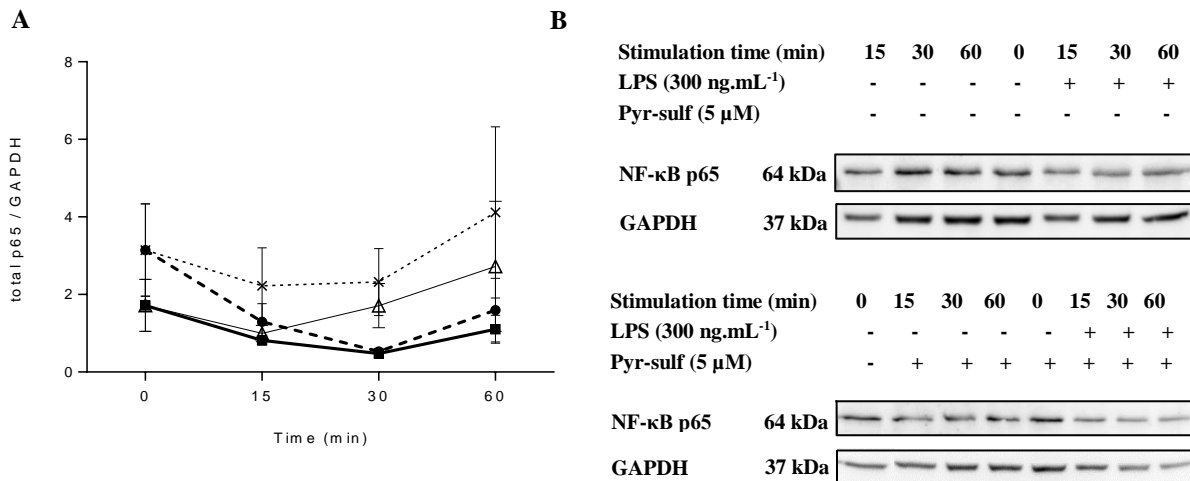
Figure 3.8. Modulation of NF-κB p65 protein levels by Pyrogallol-sulfate (Pyr-sulf) metabolite in N9 murine microglial cells stimulated with LPS. Pretreatment with Pyr-sulf was performed using a concentration of 5 µM for 6 h prior to the stimulation with LPS (300 ng.mL^{-1}) for different incubation times, 0, 15, 30 and 60 min. **(A)** Time course of the NF-κB p65 total protein levels and **(B)** representative western blots of total NF-κB p65 using GAPDH as a loading control. Black solid line with white triangles represents naïve cells without any treatment (pretreatment or LPS stimulation; negative control); Dotted line with cross symbols represents cells only treated with Pyr-sulf (positive control for metabolite); Bold solid line with squares represents LPS-stimulated cells (positive control for stimulus); Dashed line with circles represents cells pretreated with Pyr-sulf followed by stimulation with LPS. Data represent mean ± standard error of the mean (SEM) of three independent biological replicates.

The NF-κB p65 subunit is activated via phosphorylation at serine 536 of the carboxy-terminal transactivation domain (TAD). This specific residue has been previously identified as the most relevant phosphorylation site within the TAD of NF-κB p65[74,75]. Thus, we investigated phosphorylation levels at this specific residue.

In the present work, both naïve cells and (poly)phenol-treated cells exhibited the same behavior with time: NF-κB p65 phosphorylation levels were unchanged. However, a rapid increase of phosphorylation levels was clearly observed in the presence of the LPS stimulus (**Figure 3.9**). Evidence from a study in macrophage cells suggested that a LPS stimulation (500ng.mL^{-1}) for 10, 30, 60 and 120 min was able to significantly induce the phosphorylation of NF-κB p65 on serine 536[76]. Despite the differences between the macrophage cells used in that work and the microglia cells used here, the increased phosphorylation levels observed by us following 1 h of LPS stimulation is consistent with what was obtained by those authors. Interestingly, in the present study, the pretreatment with Pyr-sulf was shown to modulate NF-κB p65 phosphorylation only for the initial stages of LPS stimulation. Its effect did not persist at later time points; 30 min after the LPS stimulation the phosphorylation ratio is similar to the LPS alone condition (**Figure 3.9**).

It has gradually been accepted that the IKK complex is not only involved in the phosphorylation of the IκBα inhibitory protein but also in the phosphorylation of the p65 subunit[74,77]. This suggests that

IKK may play a crucial role in the activation of NF-κB. Although it is not totally clear which catalytic subunit of this kinase complex is involved in the phosphorylation of the nuclear transcription factor, previous research has reported an essential role for IKKβ in the phosphorylation of serine 536 following stimulation with LPS[76]. The molecular components involved in the phosphorylation of IκBα or NF-κB p65, and the corresponding mechanisms behind this process, could be key steps for the differential modulation exerted by the Pyr-sulf metabolite.

In our study, results obtained suggest that Pyr-sulf may provide more stability to IκBα protein, preventing its phosphorylation and its subsequent degradation (**Figure 3.6 and Figure 3.7**). On the other hand, phosphorylation of NF-κB p65 is less influenced by the Pyr-sulf metabolite. The only (slight and not significant) effect was observed at the initial stages of LPS stimulation (**Figure 3.9**).
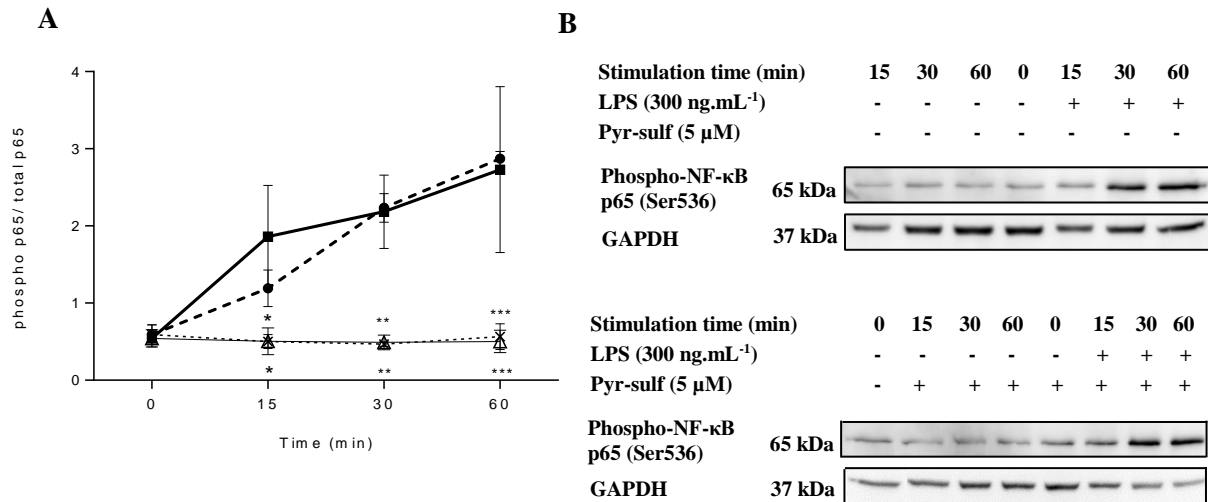
Figure 3.9. Kinetics of NF-κB p65 phosphorylation in the presence of Pyrogallol-sulfate (Pyr-sulf) metabolite in N9 murine microglial cells stimulated with LPS. Pretreatment with Pyr-sulf was performed using a concentration of 5 μM for 6 h prior to the stimulation with LPS (300 ng.mL^{-1}) for different incubation times 0, 15, 30 and 60 min. **(A)** NF-κB phosphorylation (at Ser536) ratio with time and **(B)** representative western blots of NF-κB phosphorylated state using GAPDH as a loading control. Black solid line with white triangles represents naïve cells without any treatment (pretreatment or LPS stimulation; negative control); Dotted line with cross symbols represents cells only treated with Pyr-sulf (positive control for metabolite); Bold solid line with squares represents LPS-stimulated cells (positive control for stimulus); Dashed line with circles represents cells pretreated with Pyr-sulf followed by LPS stimulation. Data represent mean ± standard error of the mean (SEM) of three independent biological replicates; Statistical differences are relative to LPS control, for each time point and pretreatment, denoted as ***$p<0.001$, **$p<0.01$ and *$p<0.05$.

Given that the phosphorylation of NF-κB is related to its transcriptional activity, it was logical to also monitor the nuclear translocation of this transcription factor by microcopy. As expected, we observed an increase of the NF-κB p65 nuclear translocation 60 min after the LPS stimulation (**Figure 3.10**). Furthermore, the treatment with Pyr-sulf alone did not affect the NF-κB p65 translocation (**Figure 3.10**). However, in Pyr-sulf pretreated cells that were subsequently stimulated by LPS for 60 min, we did not notice any difference from the LPS alone condition: NF-κB nuclear translocation does not appear to follow the trend that was observed for the IκBα phosphorylation ratio (**Figure 3.7**).

Looking at the course of events in the NF-κB signaling cascade in response to an injury, the phosphorylation of the IκBα inhibitory protein occurs earlier than the nuclear translocation of NF-κB into the nucleus[78]. This suggests that at later time points, beyond the 60 min studied here, greater differences could be observed (**Figure 3.10**). A previous study, also performed in the N9 microglial cell line, analyzed later time points following LPS stimulation ($10 \, \mu g.mL^{-1}$). Results were presented for IκBα and NF-κB phosphorylation and for NF-κB nuclear translocation. The latter was assessed 3 h after LPS stimulation even though increased levels of IκBα phosphorylation had been observed 1 h after the LPS addition[79].

Taking into account the results obtained here, we propose that the decreased levels of TNF-α 24 h after the LPS stimulation (**Figure 3.2B**) may be explained by the repression of phosphorylation of the IκBα inhibitor (**Figure 3.7**), which consequently attenuates the transcription of TNF-α target genes.

Interesting differences must be highlighted between previous research from the *Molecular Nutrition and Health Laboratory* and the present study. Particularly, the NF-κB p65 nuclear translocation results (**Figure 3.10** and [52]). Previous results described a reduction in the NF-κB p65 nuclear translocation, 60 min after treatment with LPS, in microglia cells pretreated for 6 h with Pyr-sulf[52]. This is not consistent with what was observed in the present study, where Pyr-sulf did not alter the response to a LPS stimulation (**Figure 3.10**). We hypothesize that a reason for the described discrepancies could be the differences in cellular densities used in the two studies. The present work used a higher cell density, which can affect microglia cells' perception of the surrounding environment and thus compromise its response against external stimuli such as LPS.

In general, the obtained results highlight the potential of these bioactive (poly)phenol metabolites, mainly Pyr-sulf, to influence the microglial-mediated inflammatory response. Their ability to play a complex and key role in the microglial-mediated inflammatory response was analyzed and could be clearly seen in the modulation of IκBα phosphorylation and the latter induction of TNF-α.

A

Pyr-sulf (5 µM)	-	+	+	-	+	+	-	+	+	-	+	+
LPS (300 ng.mL^{-1})	+	-	+	+	-	+	+	-	+	+	-	+
Stimulation time	0 min			15 min			30 min			60 min		

B
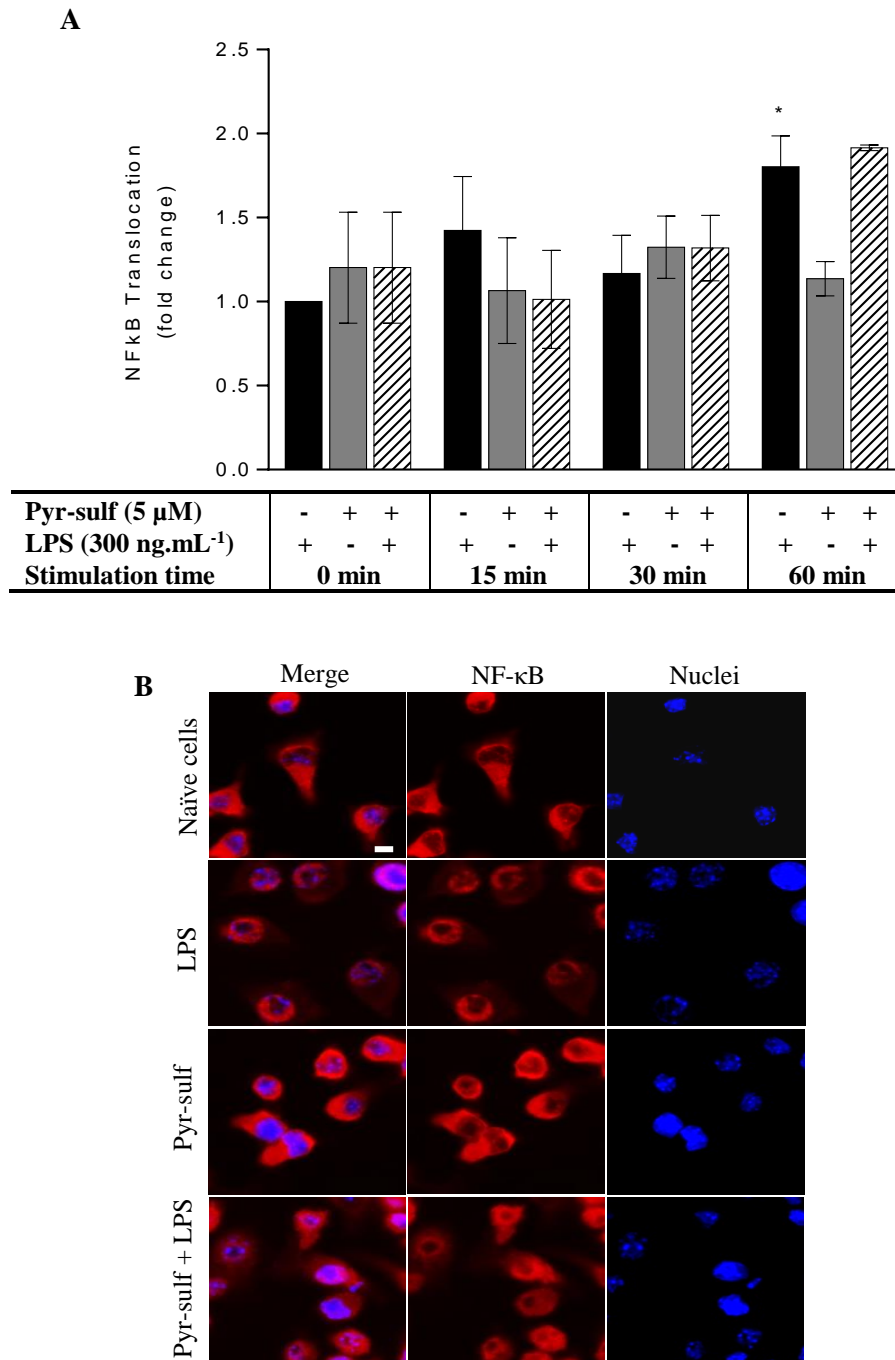
Figure 3.10. Effects of Pyrogallol-sulfate (Pyr-sulf) metabolite on NF-κB p65 translocation to the nucleus induced by LPS in N9 murine microglia cells. Pretreatment with Pyr-sulf was performed using a concentration of 5 µM for 6 h, prior to the stimulation with LPS (300 ng.mL^{-1}) for different incubation times 0, 15, 30 and 60 min. **(A)** Data obtained from the translocated and total cells ratios of different fields were normalized for the naïve control group at each time point. Black solid bars represent cells only subjected to a LPS stimulation without Pyr-sulf pretreatment (positive control); Grey solid bars represent cells only treated with Pyr-sulf; White dashed bars represent cells pretreated with Pyr-sulf followed by stimulation with LPS. Data represent mean ± standard error of the mean (SEM) of three independent biological replicates; Statistical differences are relative to LPS 0min vs 60min, denoted as *p<0.05. **(B)** Microscopy images of NF-κB p65 translocation following 60 min of LPS stimulation, representative from three independent biological replicates showing the NF-κB (red, middle panel), Nuclei stained with 4',6-diamidino-2-phenylindole (DAPI) probe (blue, right hand panel) and the overlaid images (left hand panel). Scale bar: 10 µm.

4.   CONCLUSIONS AND FUTURE PERSPECTIVES

Results from the present work provide compelling evidence that, from the human bioavailable (poly)phenols tested, Pyr-sulf is the most promising metabolite. It displayed a potential modulatory effect on neuroinflammation in a LPS-stimulated microglial cell model.

From the analysis of a set of microglial inflammatory mediators, the most prominent effect of these (poly)phenol metabolites was observed on the concentration of TNF-α. Although a 6 h Cat-sulf pretreatment with either 5 µM or 10 µM was able to reduce the production of this mediator, the strongest effect was observed for Pyr-sulf at lower concentrations (0.5 µM) and lower incubation times (4 h). Furthermore, a stimulatory effect on TNF-α protein levels was observed following 2 h of Pyr-sulf pretreatment. It is interesting to note that for 2 h incubations there is also a slight increase of TNF-α levels in response to Pyr-sulf alone. Additionally, from the analysis of the NO pro-inflammatory mediator an interesting point arose. A decrease of NO levels following 6 h of pretreatment with 0.5 µM of Cat-sulf and a subsequent LPS stimulation suggested an attenuating effect on the release of this mediator. Thus, this effect may be achieved with lower concentrations of Cat-sulf than previously thought.

The relationship between the observed protective capacity of Pyr-sulf metabolite and a pre-conditioning effect by an anti-inflammatory microglial response was clarified. The induction of an anti-inflammatory response, at least mediated by IL-4 and IL-10 cytokines at the time points investigated, is not related with the protective effect observed.

Besides the analysis of these cytokines and the NO mediator, intracellular superoxide ($O_2^{\bullet-}$) levels were also measured for both metabolites, as a crucial marker of microglial activation. While Cat-sulf pretreatment suggested a more efficient reduction of fluorescence intensity related with intracellular $O_2^{\bullet-}$ levels at 10 µM, this effect was not observed for Pyr-sulf. No clear differences in the MFI between the Pyr-sulf concentrations tested were observed. However, due to the lack of sufficient replicates we are unable to establish a statistically valid conclusion about the effect of these metabolites on this mediator under the conditions tested.

Additionally, the broadening of the study to other cellular markers involved in the activation of the NF-κB signaling pathway allowed us to conclude that the Pyr-sulf metabolite can modulate this inflammatory cascade. Following pretreatment with Pyr-sulf, the phosphorylation levels of the IκBα inhibitory protein were reduced when compared to levels from cells that only received LPS stimulation. This reduction was observed at all time points studied during LPS stimulation. Also, NF-κB p65 protein phosphorylation appears to be modulated by Pyr-sulf, though only for the initial stages of LPS stimulation.

Regarding the nuclear translocation of NF-κB p65, the observed increase in translocation following 60 min of LPS stimulation was expected, since it is a well-known inducer of the NF-κB pathway[80]. However, the Pyr-sulf pretreatment at the same time point did not result in any differences. The lack of an effect on NF-κB nuclear translocation levels, in light of the observed attenuation effect

on IκBα phosphorylation, may be a result of IκBα being upstream in the pathway and 60 min may not be sufficient to observe changes in the nuclear translocation of NF-κB. The attenuation of IκBα inhibitor phosphorylation is in agreement with the effect of Pyr-sulf on TNF-α release 24 h after LPS induction.

To summarize, our findings revealed a Pyr-sulf attenuation effect on some LPS-induced microglial markers, particularly TNF-α, IκBα and NF-κB proteins, indicating a regulatory role for Pyr-sulf on one of the main inflammatory signaling pathways. It is important to highlight that Pyr-sulf and Cat-sulf are bioavailable (poly)phenol metabolites that have previously been detected in circulation in human plasma. The use of these metabolites at physiologically relevant concentrations, and over the time ranges for which they are known to circulate, were important factors when designing this physiologically relevant study.

Although we can conclude that Pyr-sulf has a modulatory effect on IκBα inhibitor, we cannot assume that the protective effects are only mediated through this inhibitory protein. Other crucial cellular factors involved in brain inflammatory states remain to be investigated, as well as other mechanisms and pathways that could be affected by this (poly)phenol metabolite. Thus, future work should be pursued to clarify specific aspects of the Pyr-sulf mechanism of action.

One of the first tasks will be to revisit NF-κB p65 nuclear translocation, using a Pyr-sulf pretreatment and studying longer periods of LPS stimulation. Additionally, transcription analysis of: (i) IKK complex subunits (and a validation analysis of protein levels); (ii) anti-inflammatory cytokines; and (iii) NF-κB protein repressor (IκBα), should be performed to try to understand the effect of Pyr-sulf on the levels of other components of the NF-κB pathway. Moreover, the analysis of other NF-κB protein complexes, such as c-rel containing dimers, would be a point of interest in future studies. The dual NF-κB activation roles, in either neuroprotection or neuroinflammation/neurodegeneration, have been described as being dependent on the type of NF-κB dimers activated[81]. On the other hand, TLR4 has been described as a crucial immune receptor responsible for microglia activation and identified as the central responder to LPS signals[69,82]. Evidence from studies involving mutations in the *TLR4* gene confirms drastic effects on the microglial response, leading to a decrease of inflammatory products and the neurotoxicity[19,18]. TLR4 plays a crucial role in certain pathological conditions and its role in inflammation and possible mediation through metabolites will be important for future investigations. Furthermore, another pathway also described as being involved in microglia-mediated inflammation, and related with TNF-α levels, is the nuclear factor of activated T cells (NFAT)[83]. Some studies have reported and identified the expression of isoforms in microglial cells, particularly NFATc1 and NFATc2, in response to cellular calcium signaling[84,85]. NFAT signaling pathway could also be an interesting regulator to study, in order to evaluate the biological effect of Pyr-sulf in different inflammatory pathways.

Finally, the potential properties of this (poly)phenol metabolite, Pyr-sulf, should be tested in other cell models of inflammation, such as primary microglial cells, in order to validate the present findings. On the other hand, efforts must be made in the very near future to further investigate and understand the

promising beneficial effects of these diet-derived phytochemicals. In particular, their contribution to the prevention of a variety of chronic inflammation conditions, as well as a number of well-known neurodegenerative diseases.

5.   REFERENCES

1.   Ghose, A. K., Herbertz, T., Hudkins, R. L., Dorsey, B. D. & Mallamo, J. P. Knowledge-Based, Central Nervous System (CNS) Lead Selection and Lead Optimization for CNS Drug Discovery. *ACS Chem. Neurosci.* **3,** 50–68 (2012).

2.   Lehnardt, S. Innate Immunity and Neuroinflammation in the CNS : The Role of Microglia in Toll-Like Receptor-Mediated Neuronal Injury. *Glia* **58,** 253–263 (2010).

3.   Tian, L., Ma, L., Kaarela, T. & Li, Z. Neuroimmune crosstalk in the central nervous system and its significance for neurological diseases. *J. Neuroinflammation* **9,** 155 (2012).

4.   Graeber, M. B., Streit, W. J. & Pain, Á. N. Á. Microglia : biology and pathology. *Acta Neuropathol.* **119,** 89–105 (2010).

5.   Becher, B., Spath, S. & Goverman, J. Cytokine networks in neuroinflammation. *Nat. Rev.* (2016).

6.   Cherry, J. D., Olschowka, J. A. & Banion, M. K. O. Neuroinflammation and M2 microglia : the good , the bad , and the inflamed. *J. Neuroinflammation* **11,** 98 (2014).

7.   Stansley, B., Post, J. & Hensley, K. A comparative review of cell culture systems for the study of microglial biology in Alzheimer's disease. *J. Neuroinflammation* **9,** 115 (2012).

8.   Lawson, L. J., Perry, V. H., Dri, P. & Rlksn, S. G. Heterogeneity in the distribution and morphology of microglia in the normal adult mouse brain. *Neuroscience* **39,** 151–170 (1990).

9.   Michelucci, A., Heurtaux, T., Grandbarbe, L., Morga, E. & Heuschling, P. Characterization of the microglial phenotype under specific pro-inflammatory and anti-inflammatory conditions: Effects of oligomeric and fi brillar amyloid- β. *J. Neuroimmunol.* **210,** 3–12 (2009).

10.   Karperien, A., Ahammer, H. & Jelinek, H. F. Quantitating the subtleties of microglial morphology with fractal analysis. *Front. Cell. Neurosci.* **7,** 1–18 (2013).

11.   Giulian, D. & Baker, J. Characterization of Ameboid Mammalian Brain Microglia Isolated from Developing. *J. Neurosci.* **6,** 2163–2178 (1986).

12.   Song, G. J. & Suk, K. Pharmacological Modulation of Functional Phenotypes of Microglia in Neurodegenerative Diseases. *Front. Aging Neurosci.* **9,** 139 (2017).

13.   Liu, H. *et al.* N9 microglial cells polarized by LPS and IL4 show differential responses to secondary environmental stimuli. *Cell. Immunol.* **278,** 84–90 (2012).

14.   Peng, W. Neuroprotective effects of G-CSF administration in microglia-mediated reactive T cell activation in vitro. *Immunol. Res.* (2017).

15.   Hanamsagar, R., Hanke, M. L. & Kielian, T. Toll-like receptor (TLR) and Inflammasome Actions in the Central Nervous System: New and Emerging Concepts. *Trends Immunol.* **33,** 333–342 (2012).

16.   Jack, C. S. *et al.* TLR Signaling Tailors Innate Immune Responses in Human. *J. Immunol.* **175,** 4320–4330 (2005).

17.   Dimayuga, F. O. *et al.* Estrogen and brain inflammation : Effects on microglial expression of MHC, costimulatory molecules and cytokines. *J. Neuroinflammation* **161,** 123–136 (2005).

18.   Walter, S. *et al.* Role of the Toll-Like Receptor 4 in Neuroinflammation in Alzheimer's Disease. *Cell. Physiol. Biochem. Orig.* **20,** 947–956 (2007).

19.   Lehnardt, S. *et al.* Activation of innate immunity in the CNS triggers neurodegeneration through a Toll-like receptor 4-dependent pathway. *PNAS* **100,** 8514–8519 (2003).

20. Oeckinghaus, A. & Ghosh, S. The NF-kB Family of Transcription Factors and Its Regulation. (2009).

21. Pahl, H. L. Activators and target genes of Rel/NF-kB transcription factors. *Oncogene* **18,** 6853–6866 (1999).

22. Klement, J. F. *et al.* IkBa Deficiency Results in a Sustained NF-kB Response and Severe Widespread Dermatitis in Mice. *Mol. Cell. Biol.* **16,** 2341–2349 (1996).

23. Niccoli, T. & Partridge, L. Ageing as a Risk Factor for Disease. *Curr. Biol.* **22,** R741–R752 (2012).

24. Diederich, M. Live longer, drink (poly)phenols! *Cell Cycle* **11,** 4109–4114 (2012).

25. Kolonel, L. N. *et al.* Vegetables, Fruits, Legumes and Prostate Cancer: A Multiethnic Case-Control Study. *Cancer Epidemiol. Biomarkers Prev.* **9,** 795–804 (2000).

26. Feskanich, D. *et al.* Prospective Study of Fruit and Vegetable Consumption and Risk of Lung Cancer Among Men and Women. *J. Natl. Cancer Inst.* **92,** 1812–1823 (2000).

27. KJ, J. *et al.* The Effect of Fruit and Vegetable Intake on Risk for Coronary Heart Disease. *Ann. Intern. Med.* **134,** 1106–1114 (2001).

28. Morris, M. C. S., Evans, D. A. M., Tangney, C. C. P., Bienias, J. L. S. & Wilson, R. S. P. Associations of vegetable and fruit consumption with age-related cognitive change. *Neurology* **67,** 1370–1376 (2006).

29. Kang, J. H., Ascherio, A. & Grodstein, F. Fruit and Vegetable Consumption and Cognitive Decline in Aging Women. *Am. Neurol. Assoc.* **57,** 713–720 (2005).

30. Dai, Q., Borenstein, A. R., Wu, Y., Jackson, J. C. & Larson, E. B. Fruit and Vegetable Juices and Alzheimer's Disease: The Kame Project. *Am. J. Med.* **119,** 751–759 (2006).

31. Liu, L. *et al.* Protective effects of tea polyphenols on exhaustive exercise-induced fatigue, inflammation and tissue damage. *Food Nutr. Res.* **61,** (2017).

32. Carey, A. N., Gomes, S. M. & Shukitt-hale, B. Blueberry Supplementation Improves Memory in Middle-Aged Mice Fed a High-Fat Diet. *J. Agric. Food Chem.* **62,** 3972−3978 (2014).

33. Cicero, A. F. G., Caliceti, C., Fogacci, F. & Giovannini, M. Effect of apple polyphenols on vascular oxidative stress and endothelium function: a translational study. *Mol. Nutr. Food Res.* (2017).

34. Nurk, E. *et al.* Intake of Flavonoid-Rich Wine, Tea, and Chocolate by Elderly Men and Women Is Associated with Better Cognitive Test Performance. *J. Nutr.* **139,** 120–127 (2009).

35. Tsao, R. Chemistry and Biochemistry of Dietary Polyphenols. *Nutrients* **2,** 1231–1246 (2010).

36. F, I., M, R., M, D., C, I. & NS, C. Polyphenols Beyond Barriers : A Glimpse into the Brain. *Curr. Neuropharmacol.* 562–594 (2017).

37. Krikorian, R. *et al.* Blueberry Supplementation Improves Memory in Older Adults. *J. Agric. Food Chem.* **58,** 3996–4000 (2010).

38. Rodriguez-mateos, A. *et al.* Intake and time dependence of blueberry flavonoid-induced improvements in vascular function: a randomized, controlled , double-blind, crossover intervention study with mechanistic insights into biological activity. *Am. Soc. Nutr.* 1179–91 (2013).

39. Gao, X., Cassidy, A., Schwarzschild, M. A., Rimm, E. B. & Ascherio, A. Habitual intake of dietary flavonoids and risk of Parkinson disease. *Neurology* **78,** 1138–1145 (2012).

40. Possemiers, S., Bolca, S., Verstraete, W. & Heyerick, A. The intestinal microbiome: A separate organ inside the body with the metabolic potential to influence the bioactivity of botanicals. *Fitoterapia* **82,** 53–66 (2011).

41. Alminger, M. *et al.* In Vitro Models for Studying Secondary Plant Metabolite Digestion and Bioaccessibility. *Compr. Rev. Food Sci. Food Saf.* **13,** 413–436 (2014).

42. Ribalta, C., Sanchez-hernandez, J. C. & Sole, M. Hepatic biotransformation and antioxidant enzyme activities in Mediterranean fish from different habitat depths. *Sci. Total Environ.* **532,** 176–183 (2015).

43. Estrela, J. M. *et al.* Polyphenolic Phytochemicals in Cancer Prevention and Therapy: Bioavailability versus Bioefficacy. *Jounal Med. Chem.* (2017).

44. Dew, T. *et al.* Urinary metabolite profiling identifies novel colonic metabolites and conjugates of phenolics in healthy volunteers. *Mol. Nutr. Food Res.* **58,** 1414–1425 (2014).

45. Ventura, M. R., Ferreira, R. B., Williamson, G., Santos, C. N. & Pimpa, R. C. Phenolic sulfates as new and highly abundant metabolites in human plasma after ingestion of a mixed berry fruit pure British Journal of Nutrition. *Br. J. Nutr.* **113,** 454–463 (2015).

46. Rio, D. Del *et al.* Dietary (Poly)phenolics in Human Health: Structures, Bioavailability, and Evidence of Protective Effects Against Chronic Diseases. *Antioxid. Redox Signal.* **18,** 1818–1892 (2013).

47. Mullen, W., Edwards, C. A. & Crozier, A. Absorption , excretion and metabolite profiling of methyl-, glucuronyl-, glucosyl- and sulpho-conjugates of quercetin in human plasma and urine after ingestion of onions. *Br. J. Nutr.* **96,** 107–116 (2006).

48. Kuresh A. Youdim, M. Zeeshan Qaiser, David J. Begley, Catherine A. Rice-Evans, N. J. A. Flavonoid permeability across an in situ model of the blood-brain barrier. *Free Radic. Biol. Med.* **36,** 592–604 (2004).

49. Youdim, K. A. *et al.* Interaction between flavonoids and the blood – brain barrier: in vitro studies. *J. Neurochem.* **85,** 180–192 (2003).

50. Ho, L. *et al.* Identification of brain-targeted bioactive dietary quercetin-3-O-glucuronide as a novel intervention for Alzheimer's disease. *FASEB J.* **27,** (2012).

51. Gasperotti, M. *et al.* Fate of microbial metabolites of dietary polyphenols in rats: is the brain their target destination? *ACS Chem. Neurosci.* (2015).

52. Figueira, I. *et al.* Polyphenols journey through blood-brain barrier towards neuronal protection. *Sci. Rep.* **7,** 11456 (2017).

53. Hartman, R. E. *et al.* Pomegranate juice decreases amyloid load and improves behavior in a mouse model of Alzheimer's disease. *Neurobiol. Dis.* **24,** 506–515 (2006).

54. Ahmed, A. H., Subaiea, G. M., Eid, A., Li, L. & Seeram, N. P. Pomegranate Extract Modulates Processing of Amyloid-β Protein in an Aged Alzheimer's Disease Animal Model. *Curr. Alzheimer Res.* **11,** 834–843 (2014).

55. González-Sarrías, A., Núñez-Sánchez, M. A., Tomás-Barberán, F. A. & Espín, J. C. Neuroprotective Effects of Bioavailable Polyphenol-Derived Metabolites against Oxidative Stress-Induced Cytotoxicity in Human Neuroblastoma SH-SY5Y Cells. *J. Agric. Food Chem* **65,** 752–758 (2017).

56. Tavares, L. *et al.* Neuroprotective effects of digested polyphenols from wild blackberry species. *Eur. J. Nutr.* **52,** 225–236 (2013).

57. JH, J. & YJ, S. Protective effect of Resveratrol on β-amyloid-induced oxidative PC12 cell death. *Free Radic. Biol. Med.* **34,** 1100–1110 (2003).

58. Li, R., Huang, Y., Fang, D. & Le, W. (–)-Epigallocatechin Gallate Inhibits Lipopolysaccharide-Induced Microglial Activation and Protects Against Inflammation-Mediated Dopaminergic Neuronal Injury. *J. Neurosci. Res.* **78,** 723–731 (2004).

59. Zhu, L.-H., Bi, W., Qi, R. & Wang, H.-D. Luteolin Inhibits Microglial Inflammation and Improves Neuron Survival Against Inflammatio. *Int. J. Neurosci.* **121,** 329–336 (2011).

60. Chen, J. *et al.* Inhibition of iNOS gene expression by quercetin is mediated by the inhibition of I κ B kinase, nuclear factor-kappa B and STAT1, and depends on heme oxygenase-1 induction in mouse BV-2 microglia. *Eur. J. Pharmacol.* **521,** 9–20 (2005).

61. C, H. *et al.* Resveratrol mitigates lipopolysaccharide- and Aβ-mediated microglial inflammation by inhibiting the TLR4/NF-κB/STAT signaling cascade. *J. Neurochem.* **120,** 461–472 (2012).

62. Duan, L. *et al.* LPS-Induced proNGF Synthesis and Release in the N9 and BV2 Microglial Cells : A New Pathway Underling Microglial Toxicity in Neuroinflammation. *PLoS One* **8,** 73768 (2013).

63. Pearson, V. L., Rothwell, N. J. & Toulmond, S. Excitotoxic Brain Damage in the Rat Induces Interleukin-1β Protein in Microglia and Astrocytes: Correlation With the Progression of Cell Death. *Glia* **25,** 311–323 (1999).

64. Ye, S. & Johnson, R. W. Increased interleukin-6 expression by microglia from brain of aged mice. *J. Neuroimmunol.* **93,** 139–148 (1999).

65. Sanz, J. M., Virgilio, F. Di, Sanz, J. M. & Virgilio, F. Di. Kinetics and Mechanism of ATP-Dependent IL-1β Release from Microglial Cells. *J. Immunol.* **164,** 4893–4898 (2000).

66. Lu, X. *et al.* Resveratrol differentially modulates inflammatory responses of microglia and astrocytes. *J. Neuroinflammation* **7,** 46 (2010).

67. Bianco, F. *et al.* Astrocyte-Derived ATP Induces Vesicle Shedding and IL-1β Release from Microglia. *J. Immunol.* **174,** 7268–7277 (2005).

68. Wang, X. *et al.* Pseudoginsenoside-F11 (PF11) exerts anti-neuroinflammatory effects on LPS-activated microglial cells by inhibiting TLR4-mediated TAK1/IKK/NF-kB, MAPKs and Akt signaling pathways. *Neuropharmacology* **79,** 642–656 (2014).

69. Wang, X. *et al.* Gomisin A inhibits lipopolysaccharide-induced inflammatory responses in N9 microglia via blocking the NF-kB/MAPKs pathway. *Food Chem. Toxicol.* **63,** 119–127 (2014).

70. Nemetchek, M. D., Stierle, A. A., Stierle, D. B. & Lurie, D. I. The Ayurvedic plant Bacopa monnieri inhibits in fl ammatory pathways in the brain. *J. Ethnopharmacol.* (2016).

71. Colton, C. A. & Gilbert, D. L. Production of superoxide anions by a CNS macrophage, the microglia. **223,** 284–288 (1987).

72. Pei, Z. *et al.* MAC1 Mediates LPS-Induced Production of Superoxide by Microglia: The Role of Pattern Recognition Receptors in Dopaminergic Neurotoxicity. *Glia* **55,** 1362–1373 (2007).

73. Birben, E., Sahiner, U. M., Sackesen, C., Erzurum, S. & Kalayci, O. Oxidative Stress and Antioxidant Defense. *WAO J.* (2012).

74. Sakurai, H., Chiba, H., Miyoshi, H., Sugita, T. & Toriumi, W. IκB Kinases Phosphorylate NF-κB p65 Subunit on Serine 536 in the Transactivation Domain. *J. Biol. Chem.* **274,** 30353–30357 (1999).

75.   Mattioli, I. *et al.* Transient and Selective NF-κB p65 Serine 536 Phosphorylation Induced by T Cell Costimulation Is Mediated by IκB Kinase β and Controls the Kinetics of p65 Nuclear Import. *J. Immunol.* **172,** 6336–6344 (2004).

76.   Yang, F., Tang, E., Guan, K., Wang, C. & Alerts, E. IKKβ Plays an Essential Role in the Phosphorylation of RelA/p65 on Serine 536 Induced by Lipopolysaccharide. *J. Immunol.* **170,** 5630–5635 (2003).

77.   Li, Q., Estepa, G., Memet, S., Israel, A. & Verma, I. M. Complete lack of NF-κB activity in IKK1 and IKK2 double-deficient mice: additional defect in neurulation. *Genes Dev.* **14,** 1729–1733 (2000).

78.   Oeckinghaus, A. & Ghosh, S. The NF-kB Family of Transcription Factors and its Regulation. *Cold Spring Harb. Perspect. Biol.* (2009).

79.   Simmons, L. J. *et al.* Regulation of inflammatory responses by neuregulin-1 in brain ischemia and microglial cells in vitro involves the NF-kappa B pathway. *J. Neuroinflammation* 1–15 (2016).

80.   Sharif, O., Bolshakov, V. N., Raines, S., Newham, P. & Perkins, N. D. Transcriptional profiling of the LPS induced NF-κB response in macrophages. *BMC Immunol.* **8,** (2007).

81.   Srinivasan, M. & Lahiri, D. K. Significance of NF-kB as a pivotal therapeutic target in the neurodegenerative pathologies of Alzheimer's disease and multiple sclerosis. *Expert Opin. Ther. Targets* (2015).

82.   Pais, T. F. *et al.* The NAD-dependent deacetylase sirtuin 2 is a suppressor of microglial activation and brain inflammation. *EMBO J.* **32,** 2603–2616 (2013).

83.   Nagamoto-Combs, K. & K.Combs, C. Microglial phenotype is regulated by activity of the transcription factor, NFAT. *J. Neurosci.* **30,** 9641–9646 (2010).

84.   Ferrari, D., Stroh, C. & Schulze-osthoff, K. P2X 7/P2Z Purinoreceptor-mediated Activation of Transcription Factor NFAT in Microglial Cells. *J. Biol. Chem.* **274,** 13205–13210 (1999).

85.   Kataoka, A., Tozaki-Saitoh, H., Koga, Y., Tsuda, M. & Inoue, K. Activation of P2X7 receptors induces CCL3 prodution in microlgial cells through transcription factor NFAT. *J. Neurochem.* **108,** 115–125 (2009).